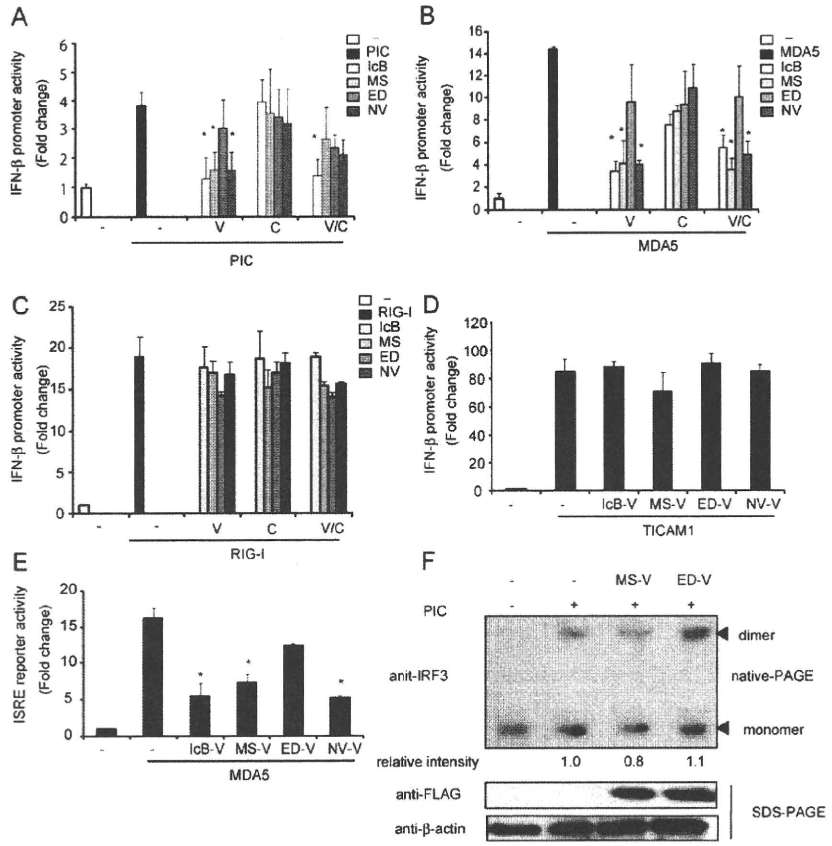

Fig. 2. Strain-to-strain difference in V protein function for MDA5-induced IFN-β promoter activation. (A) A549 cells in 24-well plates were transfected with pCMV10-MV-V (100 ng) and pCMV10-MV-C (100 ng) together with the IFN-β promoter reporter (100 ng) and phRL-TK (50 ng). Twenty-four hours after transfection, the cells were stimulated with 50 μg/ml polyI:C for 6 h, and then the luciferase reporter activity was measured. The average activities from three independent assays are shown as fold induction. A549 cells in 24-well plates were transfected with pEF-BOS FLAG-MDA5 (100 ng, B), pEF-BOS RIG-I (100 ng, C), pEF-BOS TICAM1 (100 ng, D), pCMV10-MV-V (100 ng) and pCMV10-MV-C (100 ng) together with the IFN-β promoter reporter (100 ng) and phRL-TK (50 ng). Twenty-four hours after transfection, the luciferase reporter activity was measured. (E) A549 cells in 24-well plates were transfected with pCMV10-MV-V (100 ng) and pCMV10-MV-C (100 ng) together with the ISRE luciferase gene (100 ng) and phRL-TK (50 ng). Twenty-four hours after transfection, the luciferase reporter activity was measured. The average activities from three independent assays are shown as fold induction. $^{*}p < 0.05$. (F) HeLa cells transfected with pCMV10 FLAG-MV-V (100 ng). After 24 h, cells were stimulated with 10 μg/ml polyI:C for 1 h and then lysed with native-PAGE lysis buffer or SDS-PAGE lysis buffer. For native-PAGE, the cell lysates were subjected to native-PAGE and immunoblotted with anti-IRF-3 antibody. For SDS-PAGE the cell lysates were subjected to SDS-PAGE and immunoblotted with anti-FLAG antibody or anti-β-actin (internal control). The band intensity was quantified by NIH Image J and relative band intensity was shown. The results were reproducible in three additional experiments.

tein barely suppressed polyI:C-induced IFN-β promoter activation (Fig. 2A). None of the C proteins analyzed affected IFN-β promoter activation.

PolyI:C is regarded as an analog of viral dsRNA and activates TLR3 in the endosomes and RIG-I/MDA5 in the cytoplasm. TLR3 recruits TICAM-1 while RIG-I and MDA5 recruit IPS-1 as adaptors. The two pathways converged upon NAP1, which assembles IKKε and TBK1 to activate IRF-3 and promote induction of IFN-β (Sasai et al., 2006b). Production of a trace amount of IFN-β results in amplified production of type I IFN via the IFNAR pathway, as controlled by the ISRE promoter (Takaoka and Yanai, 2006). To reveal the target pathway inhibited by the V protein of wild-type MV, we examined whether the wild-type MV V proteins block IFN-β induction in cells containing overexpressed MDA5, RIG-I or TICAM-1 (Fig. 2B–D). The V proteins of strains MS and IC-B inhibited MDA5-induced IFN-β and ISRE promoter activation but barely affected RIG-I and TICAM-1-induced IFN-β induction (Fig. 2B–E). It is notable that in our setting, V proteins of various MV strains did not suppress RIG-I-mediated activation of IFN-β promoter (Fig. 2C). These data suggested that the V proteins of wild-type strains suppress the MDA5 pathway for type I IFN induction while the C proteins barely affect MDA5-, RIG-I- and TICAM-1-dependent IFN-β transcription. Under these conditions, only the V protein of strain ED abrogates the inhibitory function of MDA5 in both IFN-β and ISRE reporters.

IRF-3 activation in the cytoplasm occurs via C-terminal phosphorylation of IRF-3 by the TBK1/NAP1/IKKε complex. These modifications promote IRF-3 homodimerization and the subsequent nuclear import of these molecules (Medzhitov, 2007; Platanias, 2005). In our studies for detection of IRF-3 dimer formation, although the V protein of the wild-type strain suppressed polyI:C-induced IRF-3 dimerization, the ED-V protein hardly inhibited polyI:C-induced IRF-3 dimerization (Fig. 2F). These data suggested that the V protein of wild-type strains inhibited polyI:C-induced IFN-β induction via the suppression of MDA5-meditaed IRF-3 activation. To exclude the possibility that the MV-V protein causes MDA5 degradation, we confirmed the MDA5 protein level by Western blotting (Fig. 3). The MDA5 protein levels in the MS-V or ED-V transfected cells were comparable to those found in untreated cells.

3.3. 272C is responsible for suppression of MDA5-induced IFN-β promoter activity

To reveal the molecular mechanism that determines whether MV V protein inhibits MDA5-induced IFN-β promoter activity, we compared the amino acid sequence of the ED V protein with that of

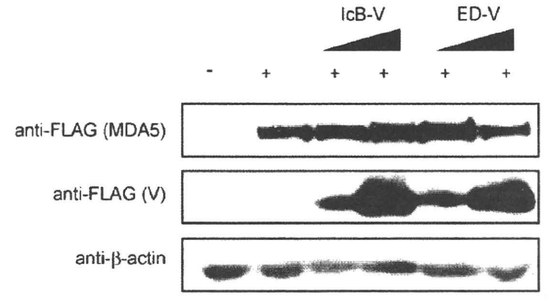

Fig. 3. Forced expression of V protein did not affect the expression level of MDA5 protein. HEK 293FT cells were transfected with pEF-BOS FLAG-MDA5 (100 ng) and pCMV10 FLAG-MV-V (10 ng, 100 ng). After 24 h, cells were lysed and subjected to Western blotting with anti-FLAG antibody and anti-β-actin antibody (internal control).

wild-type V proteins. As shown in Fig. 4, we identified 7 amino acid substitutions (51R, 83P, 97P, 110H, 225G, 272R and 291H) in the ED V protein. These conversions are ED strain V-specific, since the authentic V sequence is conserved in other strains. We then constructed R51K, P83S, P97S, H110Y, G225E, R272C and H291Y mutants of ED V protein and examined the effects of these mutants on MDA5-induced IFN-β promoter activity (Fig. 5A). As shown in Fig. 5A, only R272C mutant of ED V protein suppressed MDA5-activated IFN-β promoter. Next, we examined whether the V protein inhibited polyI:C-induced IRF-3 nuclear translocation. Although WT ED V protein did not inhibit polyI:C-induced IRF-3 nuclear translocation, overexpression of R272C mutant suppressed IRF-3 nuclear translocation (Fig. 5B and C). R51K, P83S, P97S, H110Y, G225E and H291Y mutants did not affect IRF-3 nuclear translocation. Since previous reports have shown that the V proteins of paramyxoviruses interacted with MDA5 to inhibit MDA5 activity and suppress IFN-β induction (Childs et al., 2007, 2009), we examined the interaction between MDA5 and the V proteins by immunoprecipitation. As expected, only R272C mutant interacted with MDA5, whereas WT ED V and the other mutants did not bind MDA5 (Fig. 5D). These data suggest that the arginine at position 272 in ED V protein is responsible for insuppressible activity of MDA5-induced IFN-β promoter activation. The cysteine residue at position 272 of V protein is conserved among paramyxoviruses. To clarify that 272C is important for suppressive activity of WT V protein, we examined effects of IC-B V C272R mutant on MDA5-induced IFN-β promoter activity. As shown in Fig. 6A, although IC-B V protein suppressed IFN-β promoter activity, C272R mutant was not able to inhibit IFN-β promoter activation. Similarly, C272R mutant did not suppressed poly I:C-induced IRF-3 nuclear translocation and interact with MDA5 (Fig. 6B and C). These data infer that the 272C residue of V protein is crucial for interacting with MDA5 and suppressing IRF-3 activation, which reasons that ED V strains fail to interact with MDA5.

4. Discussion

In this study, we demonstrated that the V protein of MV strain ED neither interacted with MDA5 nor suppressed MDA5-induced IRF-3 activation. A C272R mutation in the cysteine-rich region of wild-type V protein rendered the V protein IFN-insuppressible and the R272C conversion in ED strains conferred an IFN-suppressive function on the V protein. The V protein targets MDA5 and V proteins possessing the 272C residue co-precipitate with MDA5 by immunoprecipitation. Only V proteins possessing the 272C residue accelerate nuclear translocation of IRF-3. Based on the results of our reporter assay, V protein does not affect TICAM-1- or RIG-I-induced IFN-β promoter activation. Hence, the 272C residue is crucial for the V protein to block MDA5 function and MDA5 is the molecule which V protein targets for inhibition of the initial induction of IFN-β. For this reason, the ED strain used in this study allowed infected cells to induce IFN-β mRNA even in the absence of DI RNA. A previous report showed that the V protein of Sendai virus binds MDA5 via the cysteine-rich region which is conserved among paramyxoviruses (Childs et al., 2009). Accordingly, we found that the MV V protein interacted with MDA5 via the cysteine-rich region.

```
MS-V     1 MAEEQARHVKNGLECIRALKAEPIGSLAIGEAMAAWSEISDNPGQERATCKEEKAGGSGL 60
IC-B-V   1 MAEEQARHVKNGLECIRALKAEPIGSLAVEEAMAAWSEISDNPGQDRATCKEEEAGSSGL 60
NV-V     1 MAEEQARHVKNGLECIRALKAEPIGSLAIGEAMAAWSEISDNPGQERATCKEEKAGGSGL 60
ED-V     1 MAEEQARHVKNGLECIRALKAEPIGSLAIEEAMAAWSEISDNPGQERATCREEKAGSSGL 60
           ****************************: ***************:****:**:**.***

MS-V    61 SKPCLSAIGSTEGGAPRIRGQGSGESDDDTETLGIPSRNLQASSTGLQCYYVYDHSGEAV 120
IC-B-V  61 SKPCLSAIGSTEGGAPRIRGQGSGESDDDAETLGIPSRNLQASSTGLQCYHVYDHSGEAV 120
NV-V    61 SKSCLSAVGSTEGGAPRIRGQGSGESDDDTETLGIPSRNLQASSTGLQCYYVYDHSGEAV 120
ED-V    61 SKPCLSAIGSTEGGAPRIRGQGPGESDDDAETLGIPPRNLQASSTGLQCHYVYDHSGEAV 120
           **.****:**************.******:******.*************::********

MS-V   121 KGIQDADSIMVQSGLDGDSTLSGGDNESENSDVDIGEPDTEGYAITDRGSAPISMGFRAS 180
IC-B-V121 KGIQDADSIMVQSGLDGDSTLSGGDDESENSDVDIGEPDTEGYAITDRGSAPISMGFRAS 180
NV-V   121 KGIQDADSIMVQSGLDGDSTLSGGDNESENSDVDIGEPDTEGYAITDRGSAPISMGFRAS 180
ED-V   121 KGIQDADSIMVQSGLDGDSTLSGGDNESENSDVDIGEPDTEGYAITDRGSAPISMGFRAS 180
           *************************:**********************************

MS-V   181 DVETAEGGEIHELLRLQSRGNTLPKLGKTLNVPPPPDPGRASASETPIKKGHRREISLIW 240
IC-B-V181 DVETAEGGEIHELLKLQSRGNNFPKLGKTLNVPPPPNPSRASTSETPIKKGHRREIGLIW 240
NV-V   181 DVETAEGGEIHELLRLQSRGNTFPKLGKTLNVPPPPDPGRASTSETPIKKGHRREISLIW 240
ED-V   181 DVETAEGGEIHELLRLQSRGNNFPKLGKTLNVPPPPDPGRASTSGTPIKKGHRREISLIW 240
           **************:******.:**************:*. **:* ***********.***

MS-V   241 NGDRVFIDRWCNPMCSKVTLGTIRARCTCGECPRVCEQCRTDTGVDTRIWYHNLPEIPE 299
IC-B-V241 NGDRVFIDRWCNPMCSKVTLGTIRARCTCGECPRVCEQCRTDTGVDTRIWYHNLPEIPE 299
NV-V   241 NGDRVFIDRWCNPMCSKVTLGTIRARCTCGECPRVCEQCRTDTGVDTRIWYHNLPEIPE 299
ED-V   241 NGDRVFIDRWCNPMCSKVTLGTIRARCTCGERPRVCEQCRTDTGVDTRIWHHNLPEIPE 299
           ******************************* *****************:*********
```

Fig. 4. Comparison of the ED V protein amino acid sequences with various MV strain. Several point mutations were found in the ED-V protein. Underline shows the conserved-Cys-rich region. Arrow heads show mutations in ED V protein.

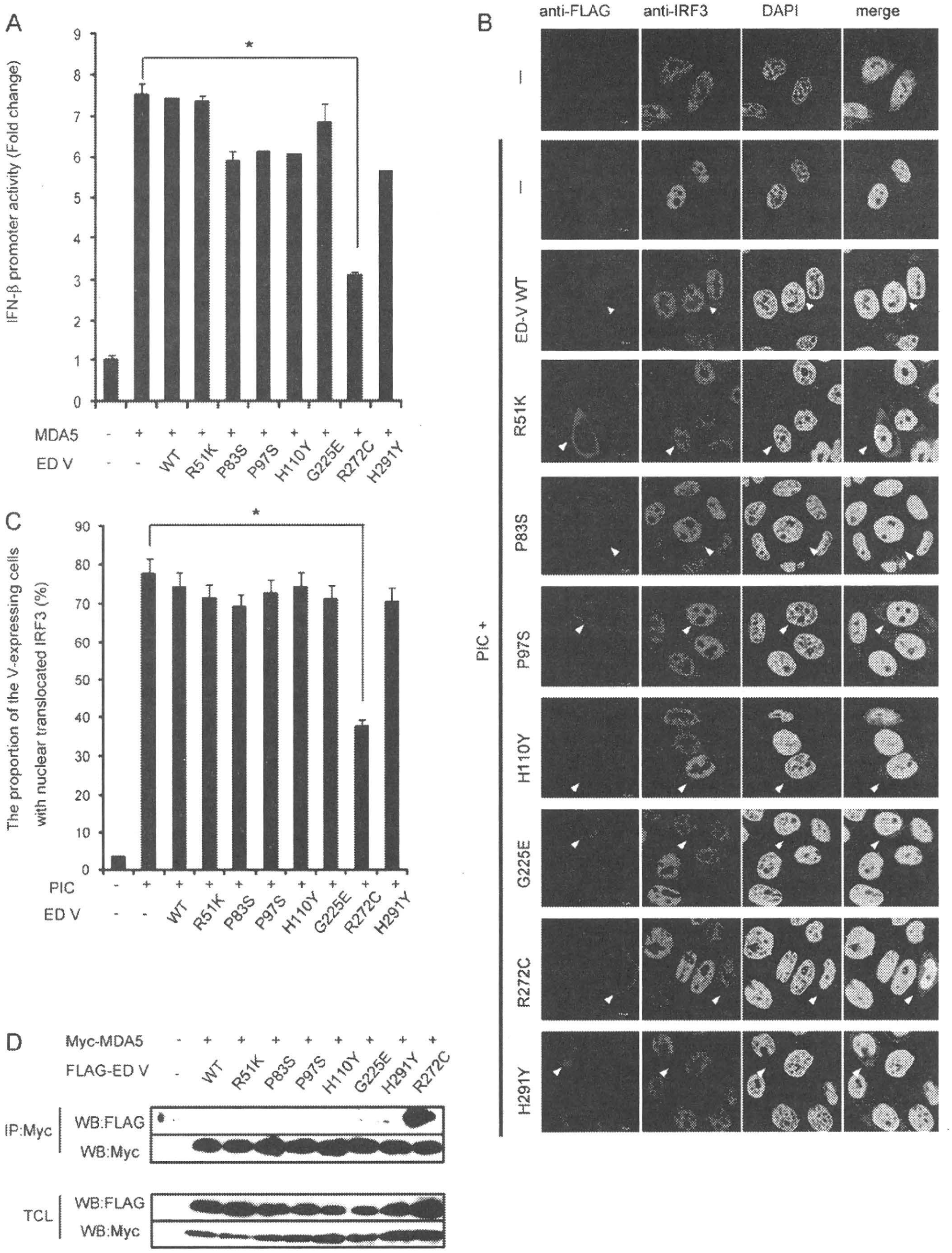

Fig. 5. 272C is a critical residue for suppression of MDA5-induced IFN-β promoter activity. (A) A549 cells in 24-well plates were transfected with pEF-BOS FLAG-MDA5 and pCMV10-MV-V together with the IFN-β promoter reporter and phRL-TK. Twenty-four hours after transfection, the luciferase reporter activity was measured. The average activities from three independent assays are shown as fold induction. *$p < 0.05$. (B) HeLa cells were transfected with various pCMV10 ED-V plasmids. After 24 h, the cells were stimulated with 10 μg/ml polyI:C for 1 h, fixed and stained with anti-IRF-3 and anti-FLAG antibodies (V protein), and visualized with either Alexa Fluor 488- or Alexa Fluor 594-conjugated secondary antibodies. The same slide was also treated with DAPI for the staining of nuclei. Arrow heads show V-expressing cells. (C) The number of the V-expressing cells with nuclear translocated IRF3 (see panel B) were counted. The results are shown by the proportion of the V-expressing cells with nuclear translocated IRF3 ($n = 50$). The average proportions from three independent assays are shown. *$p < 0.05$. (D) HEK293FT cells were transfected with pcDNA4 Myc-MDA5 and pCMV10 FLAG-MV-V with mutations. After 24 h, the cells were lysed, immunoprecipitated with anti-FLAG antibody and immunoblotted with anti-Myc or anti-FLAG antibodies. An aliquot of each total cell lysate (TCL) was immunoblotted with either anti-Myc or anti-FLAG antibodies.

Childs et al. (2009) reported that the V protein of paramyxovirus specifically inhibited activation of the MDA5 pathway, but not the RIG-I pathway, by specifically binding to the helicase domain of MDA5 and hindering MDA5 from recruiting dsRNA. Consistent with their report, the V protein thus blocks sensing dsRNA via MDA5 to disassemble oligomerization of MDA5. These results infer that the IFN-inducible properties of the laboratory-adapted ED strain were largely attributable to the aberrance of the function of the V protein by introduction of the C272R mutation. We only regret that we could not detect the complex of endogenous MDA5 and MV V in this study since resting cells express only a trace amount of MDA5 (Yoneyama et al., 2005).

Ohno et al. (2004) showed that the 110Y and 272C residues of the V protein were responsible for the suppression of IFN-α and IFN receptor signaling using HEK293 transfectants. In contrast, we clarified that C272R mutant but H110Y mutant of ED V protein sup-

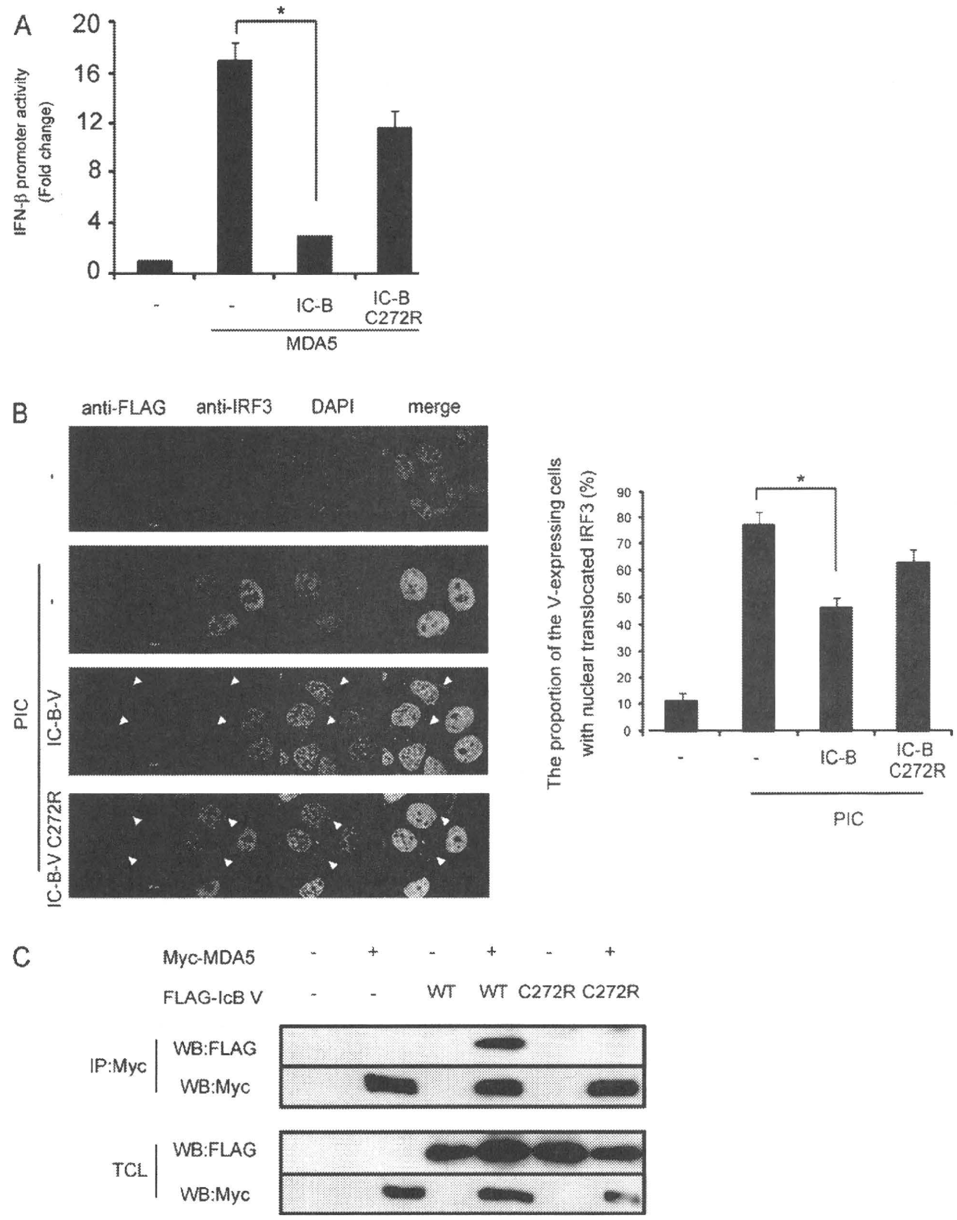

Fig. 6. 272C is important for suppressive activity of WT V protein. (A) A549 cells in 24-well plates were transfected with pEF-BOS FLAG-MDA5 and various pCMV10-IC-B-V plasmids together with the IFN-β promoter reporter and phRL-TK. Twenty-four hours after transfection, the luciferase reporter activity was measured. The average activities from three independent assays are shown as fold induction. $^*p < 0.05$. (B) HeLa cells were transfected with various pCMV10 ED-V plasmids. After 24 h, the cells were stimulated with 10 μg/ml polyI:C for 1 h, fixed and stained with anti-IRF-3 and anti-FLAG antibodies (V protein), and visualized with either Alexa Fluor 488- or Alexa Fluor 594-conjugated secondary antibodies. The same slide was also treated with DAPI for the staining of nuclei. Arrow heads show V-expressing cells. Right panel shows the proportion of the V-expressing cells with nuclear translocated IRF3. (C) Immunoprecipitation assay in 293T cells. Cells were transfected with pcDNA4 Myc-MDA5 and pCMV10 FLAG-MV-V. After 24 h, the cells were lysed, immunoprecipitated with anti-FLAG antibody and immunoblotted with anti-Myc or anti-FLAG antibodies. An aliquot of each total cell lysate (TCL) was immunoblotted with either anti-Myc or anti-FLAG antibodies.

pressed IFN-β promoter activity in the MDA5 pathway. Hence, the tyrosine at position 110 is responsible only for blocking the IFN amplification pathway via IFN-α/β receptor (IFNAR). On the other hand, the cysteine residue at position 272 is important for inhibiting both MDA5-induced IFN-β transactivation and IFNAR amplification loop. The V protein of strain ED is unable to block not only MDA5 but also the IFNAR amplification pathway, thereby ED-based vaccine strains would be able to induce type I IFN. Consistent with this possibility, Ikegame et al. (2010) reported the participation of MDA5 in MV-mediated IFN induction and MV growth promotion using RIG-I-silenced cells and V protein-deficient MV strains. In fact, the V proteins of ED and wild-type strains play no role in blocking the downstream of TBK1 for IFN-β reporter activation (data not shown). However, we wonder if the viruses produce sufficient amounts of long dsRNA (>40 bp in length, enough to be detected by J2 mAb) to be recognized by MDA5 in an early step of infection, i.e. before the production of V protein. Since RIG-I recognizes 5′-3P-ssRNA or short dsRNA, the RIG-I pathway is thought to be predominantly involved in IFN induction in MV-infected cells (Plumet et al., 2007; Shingai et al., 2007). Detailed analysis will be required to elucidate the predominant usage of RIG-I or MDA5 for type I IFN induction in cells infected with a variety of viruses. Why MV blocks MDA5 but not RIG-I activity and which viral products specifically recognize and bind MDA5 are questions that remained to be answered.

The C protein of MV plays an important role in inhibiting the JAK-STAT pathway of IFNAR signaling (Shaffer et al., 2003), and also acts as a regulator of viral RNA synthesis, thereby indirectly suppressing IFN induction (Nakatsu et al., 2006, 2008; Takeuchi et al., 2005). MV mutants that fail to express the C protein allow infected cells to generate dsRNA (Ikegame et al., 2010), suggesting that the C protein may also function in controlling the generation of long dsRNA. In this study, we observed that the forced expression of C protein did not affect polyI:C-, RIG-I- and MDA5-induced IFN-β reporter activity and there were no significant amino acid changes in this protein among wild-type and vaccine strains (data not shown). C protein appears neither to directly affect the IFN-inducing pathways, nor to be responsible for the IFN-induction of vaccine strains. An interesting issue is the relationship between activation of the MDA5 pathway by MV vaccine strains and the limited production of long dsRNA due to the function of the C protein.

In conclusion, our data suggest that the C272R mutation in the V protein in MV strains is a major cause of insuppressible IFN production in a certain case of MV infection and that the 272C residue of the V protein is responsible for the MDA5-blocking ability of wild-type MV. Although RIG-I recognizes MV products including DI RNA or 5′-3P-ssRNA, the initial response of MDA5 also acts as a cause for amplifying type I IFN production, at least in some vaccine strains.

Conflict of interest

There is no conflict of interest in this study.

Acknowledgements

We are grateful to Drs. A. Watanabe, H.H. Aly, H. Shime, J. Kasamatsu, S. Yamazaki, and T. Ebihara for invaluable discussions. This work was supported in part by Grants-in-Aid from the Ministry of Education, Science, and Culture, the Ministry of Health, Labor, and Welfare of Japan, and by the NorthTec Foundation, the Yakult Foundation, Waxman Foundation and the Akiyama Life Science Foundation. Financial support by the Sapporo Biocluster "Bio-S" the Knowledge Cluster Initiative of the MEXT, and the Program of Founding Research Centers for Emerging and Reemerging Infectious Diseases, MEXT are gratefully acknowledged.

References

Bowie, A.G., Fitzgerald, K.A., 2007. RIG-I: tri-ing to discriminate between self and non-self RNA. Trends Immunol. 28, 147–150.

Calain, P., Curran, J., Kolakofsky, D., Roux, L., 1992. Molecular cloning of natural paramyxovirus copy-back defective interfering RNAs and their expression from DNA. Virology 191, 62–71.

Childs, K., Stock, N., Ross, C., Andrejeva, J., Hilton, L., Skinner, M., Randall, R., Goodbourn, S., 2007. mda-5, but not RIG-I, is a common target for paramyxovirus V protein. Virology 359, 190–200.

Childs, K.S., Andrejeva, J., Randall, R.E., Goodbourn, S., 2009. Mechanism of mda-5 inhibition by paramyxovirus V protein. J. Virol. 83, 1465–1473.

Funami, K., Sasai, M., Oshiumi, H., Seya, T., Matsumoto, M., 2008. Homo-oligomerization is essential for Toll/IL-1 receptor domain containing adaptor molecule-1-mediated NF-kappaB and interferon regulatory factor-3 activation. J. Biol. Chem. 283, 18283–18291.

Ikegame, S., Takeda, M., Ohno, S., Nakatsu, Y., Nakanishi, Y., Yanagi, Y., 2010. Both RIG-I and MDA5 RNA helicases contribute to the induction of alpha/beta interferon in measles virus-infected human cells. J. Virol. 84, 372–379.

Katze, M.G., He, Y., Gale Jr., M., 2002. Viruses and interferon: a fight for supremacy. Nat. Rev. Immunol. 2, 675–687.

Kubune, F., Sakata, H., Hayashi, T., 1990. Marmoset lymophoblastoid cells as a sensitive host for isolation of measles virus. J. Virol. 64, 700–705.

Kurita-Taniguchi, M., Fukui, A., Hazeki, K., Hirano, A., Tsuji, S., Matsumoto, M., Watanabe, M., Ueda, S., Seya, T., 2000. Functional modulation of human macrophages through CD46 (measles virus receptor): production of IL-12p40 and nitric oxide in association with recruitment of protein-tyrosine phosphatase SHP-1 to CD46. J. Immunol. 165, 5143–5152.

Medzhitov, R., 2007. Recognition of microorganisms and activation of the immune response. Nature 449, 819–826.

Murabayashi, N., Kurita-Taniguchi, M., Ayata, M., Matsumoto, M., Ogura, H., Seya, T., 2002. Susceptibility of human dendritic cells (DCs) to measles virus (MV) depends on their activation stages in conjunction with the level of CDw150: role of Tol stimulators in DC maturation and MV amplification. Microbes Infect. 4, 785–794.

Nakatsu, Y., Takeda, M., Ohno, S., Koga, R., Yanagi, Y., 2006. Translational inhibition and increased interferon induction in cells infected with C protein-deficient measles virus. J. Virol. 80, 11861–11867.

Nakatsu, Y., Takeda, M., Ohno, S., Shirogane, Y., Iwasaki, M., Yanagi, Y., 2008. Measles virus circumvents the host interferon response by different action of the C and V proteins. J. Virol. 82, 8296–8306.

Naniche, D., Yeh, A., Eto, D., Manchester, M., Friedman, R.M., Oldstone, M.B.A., 2000. Evasion of host defenses by measles virus: wild-type measles virus infection interferes with induction of alpha/beta interferon production. J. Virol. 74, 7478–7484.

Ohno, S., Ono, N., Takeda, M., Takeuchi, K., Yanagi, Y., 2004. Dissection of measles virus V protein in relation to its ability to block alpha/beta interferon signal transduction. J. Gen. Virol. 85, 2991–2999.

Oshiumi, H., Matsumoto, M., Funami, K., Akazawa, T., Seya, T., 2003. TICAM-1, an adaptor molecule that participates in Toll-like receptor 3-mediated interferon-beta induction. Nat. Immunol. 4, 161–167.

Patterson, J.B., Thomas, D., Lewicki, H., Billeter, M.A., Oldstone, M.B., 2000. V and C proteins of measles virus function as virulence factors in vivo. Virology 267, 80–89.

Pichlmair, A., Reis, E., Sousa, C., 2007. Innate recognition of viruses. Immunity 27, 370–383.

Platanias, L.C., 2005. Mechanisms of type-I- and type-II-interferon-mediated signalling. Nat. Rev. Immunol. 5, 375–386.

Plumet, S., Herschke, F., Bourhis, J.M., Valentin, H., Longhi, S., Gerlier, D., 2007. Cytosolic 5′-triphosphate ended viral leader transcript of measles virus as activator of the RIG I-mediated interferon response. PLoS One 14, e279.

Radecke, F., Billeter, M.A., 1996. The nonstructural C protein is not essential for multiplication of Edmonsto B strain measles virus in cultured cells. Virology 217, 418–421.

Samuel, C.E., 2001. Antiviral actions of interferons. Clin. Microbiol. Rev. 14, 778–809.

Sasai, M., Shingai, M., Funami, K., Yoneyama, M., Fujita, T., Matsumoto, M., Seya, T., 2006a. NAK-associated protein 1 participates in both the TLR3 and the cytoplasmic pathways in type I IFN induction. J. Immunol. 177, 8676–8683.

Sasai, M., Matsumoto, M., Seya, T., 2006b. The kinase complex responsible for IRF-3-mediated IFN-{beta} production in myeloid dendritic cells (mDC). J. Biochem. (Tokyo) 139, 171–175.

Sen, G.C., 2001. Viruses and interferons. Annu. Rev. Microbiol. 55, 255–281.

Shaffer, J.A., Bellini, W.J., Rota, P.A., 2003. The C protein of measles virus inhibits the type I interferon response. Virology 315, 389–397.

Shingai, M., Ebihara, T., Begum, N.A., Kato, A., Honnma, T., Matsumoto, K., Saito, H., Ogura, H., Matsumoto, M., Seya, T., 2007. Differential type I IFN-inducing abilities of wild-type versus vaccine strains of measles virus. J. Immunol. 179, 6123–6133.

Sidhu, M.S., Crowley, J., Lowenthal, A., Karcher, D., Menonna, J., Cook, S., Udem, S., Dowling, P., 1994. Defective measles virus in human subacute sclerosing panencephalitis brain. Virology 202, 631–641.

Takaoka, A., Yanai, H., 2006. Interferon signalling network in innate defence. Cell Microbiol. 8, 907–922.

Takeuchi, O., Akira, S., 2008. MDA5/RIG-I and virus recognition. Curr. Opin. Immunol. 20, 17–22.

Takeuchi, K., Kadota, S.I., Takeda, M., Miyajima, N., Nagata, K., 2003. Measles virus V protein blocks interferon (IFN)-alpha/beta but not IFN-gamma signaling by inhibiting STAT1 and STAT2 phosphorylation. FEBS Lett. 545, 177–182.

Takeuchi, K., Takeda, M., Miyajima, N., Ami, Y., Nagata, N., Suzuki, Y., Shahnewaz, J., Kadota, S., Nagata, K., 2005. Stringent requirement for the C protein of wild-type measles virus for growth both in vitro and in macaques. J. Virol. 79, 7838–7844.

Tanabe, M., Kurita-Taniguchi, M., Takeuchi, K., Takeda, M., Ayata, M., Ogura, H., Matsumoto, M., Shingai, M., Ayata, M., Ogura, M., Seya, T., 2003. Mechanism of up-regulation of human Toll-like receptor 3 secondary to infection of measles virus-attenuated strains. Biochem. Biophys. Res. Commun. 311, 39–48.

Whistler, T., Bellini, W.J., Rota, P.A., 1996. Generation of defective interfering particles by two vaccine strains of measles virus. Virology 220, 480–484.

Yoneyama, M., Kikuchi, M., Matsumoto, K., Imaizumi, T., Miyagishi, M., Taira, K., Foy, E., Loo, Y.M., Gale Jr., M., Akira, S., Yonehara, S., Kato, A., Fujita, T., 2005. Shared and unique functions of the DExD/H-box helicases RIG-I, MDA5, and LGP2 in antiviral innate immunity. J. Immunol. 175, 2851–2858.

balt3/zbc-bc/zbc-bc/zbc01711/zbc5609-11z ZSUBMIT 9 xppws S=1 10/2/11 11:08 4/Color Figure(s) F3,4,6,7 ARTNO: M110.185793

THE JOURNAL OF BIOLOGICAL CHEMISTRY VOL. 286, NO. ??, pp. 1–xxx, ???? ??, 2011

Raftlin Is Involved in the Nucleocapture Complex to Induce Poly(I:C)-mediated TLR3 Activation*[S]

Received for publication, September 15, 2010, and in revised form, January 23, 2011 Published, JBC Papers in Press, January 25, 2011, DOI 10.1074/jbc.M110.185793

Ayako Watanabe[‡], Megumi Tatematsu[‡], Kazuko Saeki[§], Sachiko Shibata[¶], Hiroaki Shime[‡], Akihiko Yoshimura[||], Chikashi Obuse[¶], Tsukasa Seya[‡], and Misako Matsumoto[‡1]

From the [‡]Department of Microbiology and Immunology, Hokkaido University Graduate School of Medicine, Kita 15, Nishi 7, Kita-ku, Sapporo 060-8638, the [§]Department of Medical Biochemistry, Graduate School of Medical Sciences, Kyushu University, Fukuoka 812-8582, the [¶]Division of Molecular Life Science, Graduate School of Life Science, Hokkaido University, Sapporo 001-0021, and the [||]Department of Microbiology and Immunology, School of Medicine, Keio University, Tokyo 160-8582, Japan

AQ: A

The double-stranded RNA analog, poly(I:C), extracellularly activates both the endosomal Toll-like receptor (TLR) 3 and the cytoplasmic RNA helicase, melanoma differentiation-associated gene 5, leading to the production of type I interferons (IFNs) and inflammatory cytokines. The mechanism by which extracellular poly(I:C) is delivered to TLR3-positive organelles and the cytoplasm remains to be elucidated. Here, we show that the cytoplasmic lipid raft protein, Raftlin, is essential for poly(I:C) cellular uptake in human myeloid dendritic cells and epithelial cells. When Raftlin was silenced, poly(I:C) failed to enter cells and induction of IFN-β production was inhibited. In addition, cellular uptake of B-type oligodeoxynucleotide that shares its uptake receptor with poly(I:C) was suppressed in Raftlin knockdown cells. Upon poly(I:C) stimulation, Raftlin was translocated from the cytoplasm to the plasma membrane where it colocalized with poly(I:C), and thereafter moved to TLR3-positive endosomes. Thus, Raftlin cooperates with the uptake receptor to mediate cell entry of poly(I:C), which is critical for activation of TLR3.

Fn2

Polyriboinosinic:polyribocytidylic acid (poly(I:C)),[2] a synthetic double-stranded RNA (dsRNA), has been used as a potent type I interferon (IFN-α/β) inducer in both *in vitro* and *in vivo* studies since the discovery of anti-viral activity of type I IFNs (1–3). Many types of cells including fibroblasts, epithelial cells, and myeloid dendritic cells (DCs), produce IFN-β upon stimulation with poly(I:C). Studies have demonstrated that extracellular poly(I:C) is recognized by Toll-like receptor (TLR) 3 and cytoplasmic RNA helicase, melanoma differentiation-associated gene 5 (MDA5), and induces innate immune responses including the production of type I IFNs and inflammatory cytokines (4–8). More recently, experimental evidence has accumulated that poly(I:C) acts as an adjuvant that enhances antibody production, natural killer cell activation, and cytotoxic T lymphocyte induction through the activation of TLR3 and/or MDA5 (9–15).

Human TLR3 localizes to the endosomal compartments in myeloid DCs, whereas it localizes to both the cell surface and endosomes of fibroblasts, macrophages, and epithelial cells (5, 16, 17). TLR3 signaling arises from an intracellular compartment in both cell types and requires endosomal maturation. After dsRNA recognition, endosomal TLR3 recruits an adaptor molecule, *i.e.* Toll-IL-1 receptor domain-containing adaptor molecule-1 (TICAM-1, also called TRIF) that activates the NF-κB, IRF-3, and AP-1 transcription factors, leading to IFN-β production (18, 19). Also, extracellular poly(I:C) is sensed by MDA5 in the cytoplasm, resulting in the activation of IRF-3 and NF-κB via the mitochondrial outer membrane protein IPS-1 (also called MAVS, Cardif, or VISA) (20–23). However, the mechanism by which poly(I:C) is delivered from the extracellular fluid to the intracellular dsRNA sensors remains unresolved. AQ: B

A recent study showed that CD14 directly binds to poly(I:C) and mediates poly(I:C) cellular uptake (24). Bone marrow-derived macrophages from CD14-deficient mice exhibited impaired, but not completely diminished, responses to poly(I:C). Also, a class A scavenger receptor was identified as a cell surface receptor for poly(I:C) in human epithelial cells, although the response of poly(I:C) was only partially impaired in scavenger receptor A-deficient mice (25). These results suggest that an unidentified cell surface molecule mediates cell entry of poly(I:C). Indeed, we and others demonstrated that poly(I:C) is internalized into CD14-negative human myeloid DCs and HEK293 cells via clathrin-dependent endocytosis, and B- and C-type oligodeoxynucleotides (ODNs) share the uptake receptor with poly(I:C) (26–28).

In this study, we isolated poly(I:C)-binding proteins from CD14-negative cell lysates by sequential affinity chromatography with poly(U)- and poly(I:C)-Sepharose and subjected them to mass spectrometric analysis. Among the proteins identified, we selected several proteins that exhibited a transmembrane domain or a membrane-anchoring motif and examined whether they were involved in poly(I:C)-induced TLR3-mediated signaling. We found that Raftlin, a major lipid raft protein

* This work was supported in part by Grants-in-aid from the Ministry of Education, Science, and Culture, the Ministry of Health, Labor, and Welfare of Japan, and the Akiyama Foundation, NorthTec Foundation, Yakult Foundation, and the Program of Founding Research Centers for Emerging and Reemerging Infectious Diseases, MEXT.

ZSI [S] The on-line version of this article (available at http://www.jbc.org) contains supplemental Tables S1–S3 and Figs. S1–S4.

[1] To whom correspondence should be addressed. Tel.: 81-11-706-6056; Fax: 81-11-706-7866; E-mail: matumoto@pop.med.hokudai.ac.jp.

[2] The abbreviations used are: poly(I:C), polyriboinosinic:polyribocytidylic acid; 4F2, 4F2 cell-surface antigen heavy chain; DCs, dendritic cells; BMDC, bone marrow-derived DC; CTXB, cholera toxin subunit B; MDA5, melanoma differentiation-associated gene 5; MβCD, methyl-β-cyclodextrin; MoDC, monocyte-derived immature DC; ODN, oligodeoxynucleotide; TICAM-1, Toll-IL-1 receptor-containing adaptor molecule-1; TLR, Toll-like receptor.

expressed by B cells, plays a critical role in poly(I:C) cellular uptake in human myeloid DCs and epithelial cells.

EXPERIMENTAL PROCEDURES

Cell Culture and Reagents—Human B cell lines Raji, BALL-1, and Namalwa were obtained from the Riken Cell Bank (Tukuba, Japan) and maintained in RPMI 1640 supplemented with 10% heat-inactivated FCS (BioSource Intl., Inc.) and antibiotics. HEK293 cells were obtained from Sumitomo Pharmaceuticals Co., Ltd. (Osaka, Japan) and maintained in Dulbecco's modified Eagle's medium low glucose (Invitrogen) supplemented with 10% heat-inactivated FCS and antibiotics. HeLa cells were kindly provided by Dr. T. Fujita (Kyoto University) and maintained in Eagle's minimal essential medium (Nissui, Tokyo, Japan) supplemented with 1% L-glutamine and 10% heat-inactivated FCS. Human monocyte-derived immature DCs (MoDCs) were generated from $CD14^+$ monocytes by culturing for 6 days in the presence of 500 units/ml of granulocyte-macrophage colony-stimulating factor and 100 units/ml of IL-4 (PeproTech). Bone marrow-derived DCs (BMDCs) were prepared as described (10). Polymyxin B, 4′,6-diamidine-2′-phenylindole dihydrochloride (DAPI), saponin, and methyl-β-cyclodextrin (MβCD) were purchased from Sigma. Poly(I:C) was from Amersham Biosciences, FITC-labeled ODN2006 was from InvivoGen, Alexa Fluor 488/cholera toxin subunit B (CTXB) and Alexa Fluor 568/transferrin were from Molecular Probes. MALP-2 was obtained from Biosynthesis (Nagoya, Japan). In addition, the following antibodies were used in this study: anti-dsRNA mAb (K1) (BioLink), anti-β actin mAb (Sigma), anti-clathrin heavy chain mAb (TD.1) (Santa Cruz Biotechnology), anti-Rab5 mAb (Abcam), anti-LAMP1 (H4A3) (BioLegend), HRP-conjugated secondary Abs (BIOSOURCE), FITC-labeled goat anti-mouse IgG (American Qualex), and Alexa Fluorp®-conjugated secondary antibodies (Invitrogen). Anti-human Raftlin polyclonal antibody was prepared as described (29). Anti-human TLR3 mAb (clone TLR3.7) was generated in our laboratory (5). Texas Red-labeled poly(I:C) was prepared using the 5′ EndTag™ Nucleic Acid Labeling System (Vector Laboratories, Burlingame, CA) according to the manufacturer's instructions.

AQ: C

Mice—Raftlin$^{-/-}$ mice were provided by Dr. A. Yoshimura (Keio University). Mice were maintained under specific pathogen-free conditions in the animal facility of the Hokkaido University Graduate School of Medicine. Animal experiments were performed according to the guidelines established by the Hokkaido University Animal Care and Use Committee.

Plasmids—The cDNA fragment encoding the ORF of human TLR2 or TLR3 was amplified by RT-PCR from total RNA prepared from MoDCs, and was ligated into the cloning site of the expression vector pEF-BOS, a gift from Dr. S. Nagata (Kyoto University) (5). Complementary DNA for human Raftlin was generated by PCR from cDNA derived from Raji cells using specific primers (forward primer, 5′-CTCGAGGCCGCCACCATGGGTTG-3′; reverse primer, 5′-GGATCCTTGTTTTCTTCAACCGTACCAAGCTC-3′), and was ligated into the cloning site of the expression vector pEYFP-N1 (C-terminal yellow fluorescent protein (YFP) tag, Clontech).

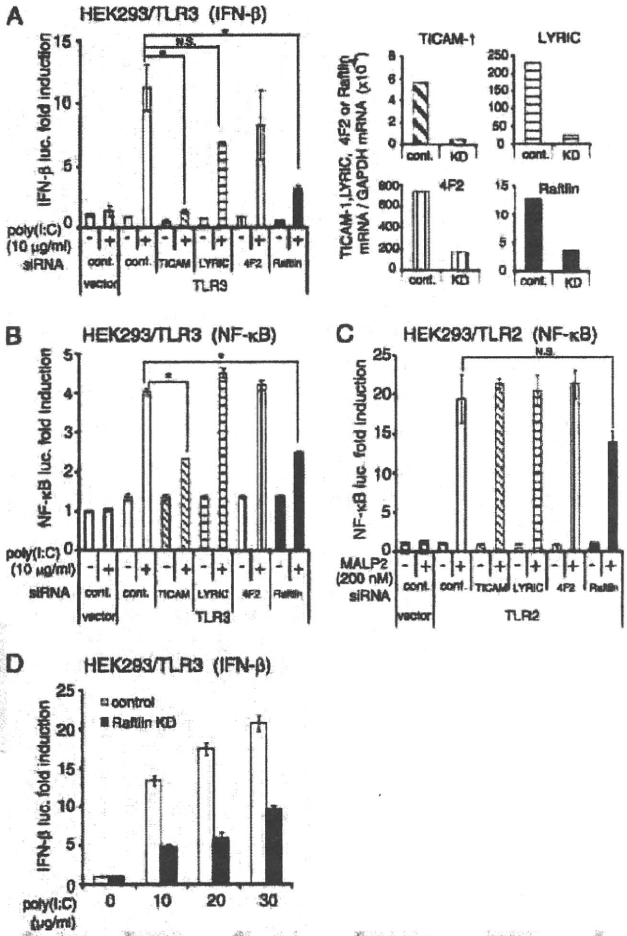

FIGURE 1. **Raftlin participates in poly(I:C)-induced TLR3-mediated signaling.** HEK293 cells were transfected with the indicated siRNAs (20 pmol) together with the expression vector for human TLR3 (*A*, *B*, and *D*), human TLR2 (*C*), or empty vector and reporter plasmid. Forty-eight hours after transfection, cells were washed and stimulated with 10–30 μg/ml of poly(I:C) or 200 nM MALP-2. After 6 h, the luciferase reporter activities were measured and expressed as fold-induction relative to the activity of unstimulated vector-transfected cells. Representative data from a minimum of three separate experiments are shown (mean ± S.D.). In each experiment, knockdown (*KD*) efficiency was assessed 48 h after transfection by qPCR. Expression of each gene was normalized to GAPDH mRNA expression. As shown in the *right-hand panels* of *A*, expression of the indicated genes is efficiently silenced (knockdown efficiency: TICAM-1, 91.4%; LYRIC, 89.5%; 4F2, 77.4%; Raftlin, 71.8%). *, $p < 0.05$ (*t* test).

Isolation of Poly(I:C)-binding Proteins—Raji cells (1×10^{10}) were washed twice with Dulbecco's phosphate-buffered saline, frozen and thawed three times in Dulbecco's phosphate-buffered saline (5×10^7/ml), and centrifuged at 20,000 × *g* for 10 min. Cell pellets were lysed in lysis buffer (1% Nonidet P-40 in buffer A (20 mM Tris-HCl, pH 7.4, 140 mM NaCl, 25 mM IAA, 10 mM EDTA, 2 mM PMSF and protease inhibitor mixture)) for 20 min at room temperature. After centrifugation at 10,000 × *g* for 10 min, supernatants were filtrated with Minisalt GF (Zartorius stedim, Japan) and sequentially applied to Sepharose, poly(U)-Sepharose, and poly(I:C)-Sepharose equilibrated with binding buffer (0.2% Nonidet P-40 in buffer A). The poly(I:C)-binding molecules were eluted from poly(I:C)-Sepharose with elution buffer (1.4 M NaCl in washing buffer) after being washed with washing buffer (10 mM CHAPS in buffer A). The eluates were AQ: D

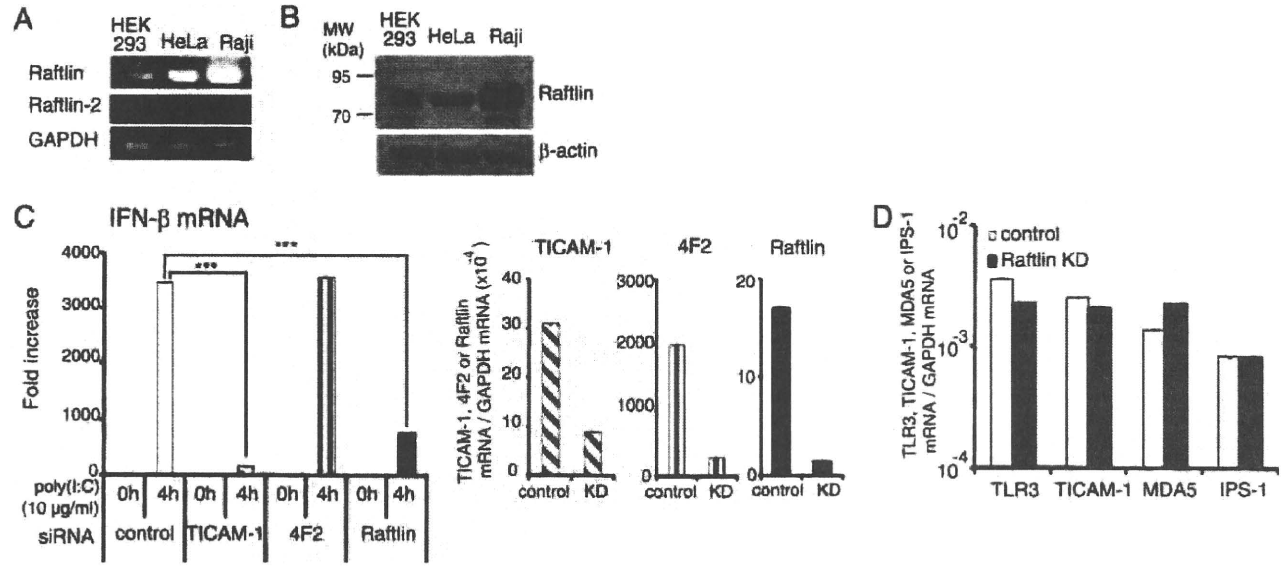

FIGURE 2. **Raftlin is essential for poly(I:C)-induced IFN-β production in HeLa cells.** *A*, expression of Raftlin and Raftlin-2 mRNAs in human cell lines. *B*, protein expression level of Raftlin in human cell lines. Cell lysates (3 μg) were separated on 10% SDS-PAGE, followed by immunoblotting with anti-Raftlin pAb or anti-β-actin mAb. *C*, poly(I:C)-induced IFN-β mRNA expression in HeLa cells. HeLa cells were transfected with the indicated siRNAs (20 pmol) using Lipofectamine 2000. Forty-eight hours after transfection, cells were washed and stimulated with 10 μg/ml of poly(I:C) for 4 h (*left-hand panel*). Total RNA was extracted and qPCR was performed using primers for the respective genes (*C* and *D*). Expression of each gene was normalized to GAPDH mRNA expression. Data are shown as the mean ± S.D., although the values are too small to represent. Representative data from three independent experiments are shown. ***, $p < 0.001$.

mixed with new poly(U)-Sepharose and rotated for 1 h at 4 °C. After centrifugation, supernatants were mixed with new poly(I:C)-Sepharose. The poly(U)- and poly(I:C)-Sepharose were washed three times with 5 volumes of washing buffer and binding molecules were eluted with elution buffer. The eluates were concentrated using YM-50 Microcon (Millipore).

Mass Spectrometry—The poly(U)- or poly(I:C)-binding molecules were separated on a 10% SDS-PAGE gel under reducing conditions, and the region of the gels containing proteins from about 250,000 to 20,000 was cut at about 1–2-mm intervals as described previously (30). After in-gel digestion with modified trypsin, the resulting peptides were analyzed by LC/MS/MS. The ion spectrum data generated by LC/MS/MS were screened against the international protein index human data base (version 3.29) with Mascot (Matrix Science, London, UK) to identify high-scoring proteins.

AQ: E

RNA Interference and Luciferase Reporter Assay—siRNA duplexes (LYRIC, catalog number s40866; 4F2, catalog number s12944; Raftlin, catalog numbers s23219, s23217, and s23218; negative control, catalog number AM4635) were obtained from Ambion-Applied Biosystems. siRNA for TICAM-1 was purchased from Xeragon Inc. (Birmingham, AL) (18). HEK293 cells cultured in 24-well plates were transfected with 20 pmol of each siRNA together with the expression vector for human TLR3 or TLR2 (200 ng), IFN-β promoter or ELAM reporter plasmid (60 ng), and an internal control vector (1.5 ng) using Lipofectamine 2000. Forty-eight hours after transfection, cells were washed once and then stimulated with 10 μg/ml of poly(I:C) or MALP-2 (200 nM) for 6 h. Cells were lysed and dual luciferase activities were measured according to the manufacturer's instructions (Promega). The *Firefly* luciferase activity was normalized to the *Renilla* activity and expressed as the fold-induction relative to the activity of unstimulated vector-transfected cells. In the case of HeLa cells, cells in 24-well plates were transfected with 20 pmol of each siRNA using Lipofectamine 2000. Knockdown of Raftlin in human MoDCs was preformed by electroporation as described previously (31). Briefly, MoDCs (1.4×10^6/80 μl) were transfected with control siRNA or siRNA for Raftlin (500 pmol) using a Gene-Pulser (Bio-Rad) and then cultured for 36 h in the presence of 500 milliunits/ml of granulocyte-macrophage colony-stimulating factor. The viability of the cells transfected with control and Raftlin siRNAs was 84 and 87%, respectively. Knockdown of mouse Raftlin-2 in Raftlin$^{-/-}$ BMDCs was performed with shRNA lentiviral particles (Santa Cruz) according to the manufacturer's instructions. Briefly, Raftlin$^{-/-}$ BMDCs in 24-well plates were infected with control shRNA lentiviral particles or mouse Raftlin-2 shRNA lentiviral particles at a multiplicity of infection of 2 and incubated in complete medium containing Polybrene (5 μg/ml). Twenty-four hours after infection, medium was replaced with complete medium and cells were further incubated for 24 h. The viability of the cells infected with control lentivirus and mouse Raftlin-2 shRNA-expressing lentivirus was 82 and 76%, respectively.

Quantitative PCR (qPCR)—Total RNA was extracted with the RNeasy mini kit (Qiagen, Valencia, CA) and 0.5 μg of RNA was reverse-transcribed using the high capacity cDNA Reverse Transcripition kit (Applied Biosystems) with random primers according to the manufacturer's instructions. Quantitative PCR was performed with the indicated primers (supplemental Table S1) using the Step One Real-time PCR system (Applied Biosystems). ZSI

Immunoblotting—Cells were lysed in lysis buffer (20 mM Tris-HCl, pH 7.4) containing 150 mM NaCl, 1% Nonidet P-40, 10 mM EDTA, 25 mM iodoacetamide, 2 mM PMSF and a protease inhibitor mixture (Roche Applied Science). Lysates were clarified by centrifugation and subjected to SDS-PAGE (10% gel) under reducing conditions, followed by immunoblotting with anti-Raftlin pAb or anti-β actin mAb.

Immunoprecipitation—HeLa cells were stimulated with 40 μg/ml of poly(I:C) for 30 min at 37 °C. At timed intervals, cells were lysed in lysis buffer for 30 min on ice. Lysates were precleared with protein G-Sepharose (GE Healthcare) and incubated with 1 μg of anti-clathrin heavy chain mAb. Immunocomplexes were recovered by incubation with Protein G-Sepharose, washed once with lysis buffer, and resuspended in denaturing buffer. Samples were analyzed by SDS-PAGE (10% gel) under reducing conditions, followed by immunoblotting with anti-Raftlin pAb (1:1000) and HRP-conjugated secondary Ab. The membrane was re-probed with anti-clathrin heavy chain mAb (1:400).

Confocal Microscopy—HeLa cells (1×10^5 cells/well) were plated onto micro coverglasses (Matsunami Glass) in 12-well plates. The next day, cells were incubated with 40 μg/ml of poly(I:C) for 30 min at 4 °C. Cells were washed once and further incubated for 5–30 min at 37 °C. At timed intervals, cells were fixed with 4% paraformaldehyde for 30 min and permeabilized with PBS containing 0.5% saponin and 1% BSA for 30 min. Fixed cells were blocked in PBS containing 1% BSA and labeled with anti-Raftlin pAb (1:500), anti-human TLR3 mAb (20 μg/ml), or Alexa Fluor 488-CTXB (10 μg/ml) for 60 min at room temperature. Alexa Fluor 488- or Alexa Fluor 568-conjugated secondary Abs (1:400) were used to visualize the primary Abs. Nuclei were stained with DAPI (2 μg/ml) in PBS for 10 min before mounting onto glass slides using PBS containing 2.3% DABCO and 50% glycerol. Cells were visualized at a ×63 magnification with an LSM510 META microscope (Zeiss, Jena, Germany).

AQ: F For uptake study, HeLa cells or HEK293 cells transfected with control siRNA or siRNA for Raftlin were incubated with 40 μg/ml of Texas Red/poly(I:C), Alexa Fluor 568/transferrin (25 μg/ml), or FITC/ODN2006 (40 μg/ml) for 30 min at 4 °C. After washing, cells were further incubated at 37 °C. At timed intervals, fixed cells were visualized as described above. In the case of HEK293 cells, cells (1×10^5 cells/well) were plated onto poly-L-lysine-coated glass (BD Bioscience) in a 24-well plate and cultured for 12 h.

Control or Raftlin knockdown MoDCs (2×10^5/100 μl) were incubated with 40 μg/ml of Texas Red/poly(I:C) for 30 min at 4 °C, washed once, and then incubated for 5–30 min at 37 °C. At timed intervals, cells were fixed with 4% paraformaldehyde for 15 min and centrifuged by Cytospin3 (Shandon). After mounting with ProLong Gold with DAPI (Molecular Probes), cells were visualized by confocal microscopy. In some experiments, MoDCs were pretreated with 1 mM MβCD for 1 h at 37 °C. Viability of cells treated with MβCD was 93.3%. For staining of endosomes, fixed cells were permeabilized with PBS containing 0.5% saponin and 1% BSA for 30 min (staining of TLR3 and early endosome), or PBS containing 100 μg/ml of digitonin and 1% BSA for 30 min (staining of late endosome). After blocking, cells were labeled with anti-Raftlin pAb (1:500), anti-human TLR3 mAb (20 μg/ml), anti-Rab5 mAb (4 μg/ml), or anti-LAMP1 mAb (H4A3) (1:200) for 60 min at room temperature.

Flow Cytometry—Cells were incubated with the indicated concentrations of poly(I:C) in culture medium for 30 min at 4 °C. After washing, cells were labeled with anti-dsRNA mAb

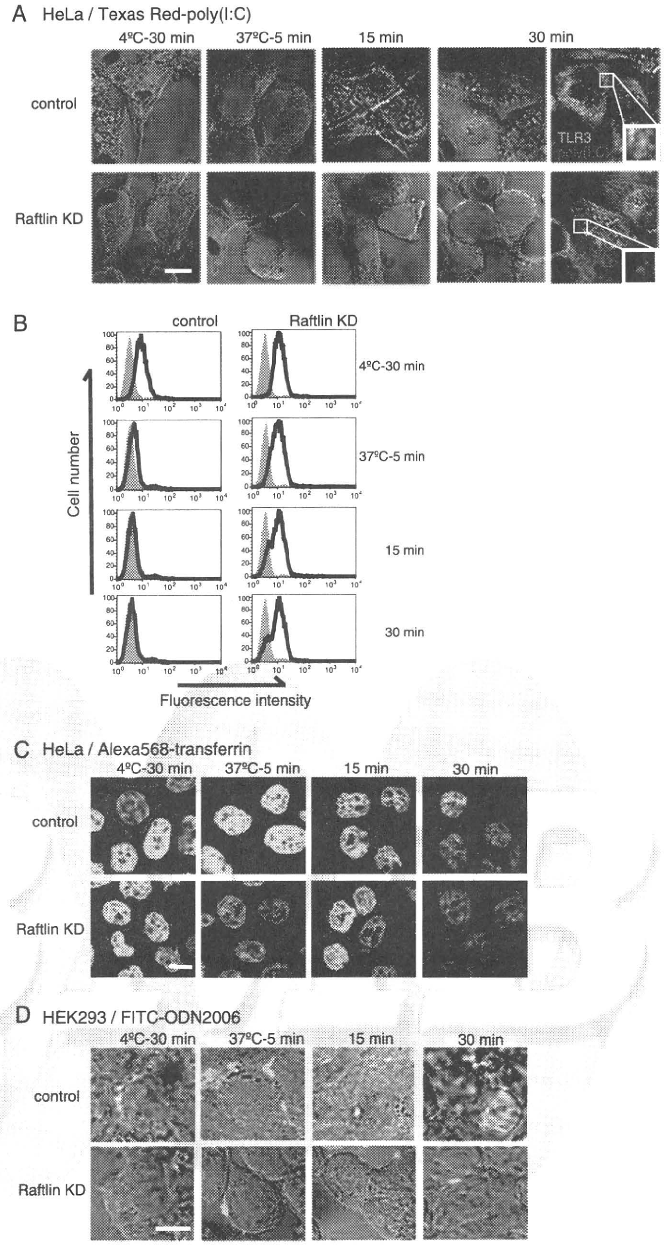

COLOR

FIGURE 3. **Knockdown of Raftlin suppresses cellular uptake of poly(I:C) and B-type ODN but not transferrin.** HeLa cells (*A* and *C*) and HEK293 cells (*D*) were transfected with control siRNA (*upper panels*) or siRNA for Raftlin (*lower panels*). Forty-eight hours after transfection, cells were washed and incubated with 40 μg/ml of Texas Red/poly(I:C) (*A*), 25 μg/ml Alexa Fluor 568/transferrin (*C*), or 40 μg/ml of FITC/ODN2006 (*D*) for 30 min at 4 °C. After washing, cells were incubated for up to 30 min at 37 °C. At timed intervals, cells were fixed and visualized by confocal microscopy. In some experiments, cells were fixed or permeabilized and stained with anti-TLR3 mAb. *A*, *red*, Texas Red-poly(I:C); *green*, TLR3. *C*, *red*, Alexa 568/transferrin; *blue*, nuclei with DAPI. *D*, *green*, FITC/ODN2006. *Bar*, 10 μm. *B*, flow cytometric analysis of poly(I:C) uptake. Control and Raftlin knockdown HeLa cells were incubated with 20 μg/ml of poly(I:C) for 30 min at 4 °C. After washing, cells were incubated for up to 30 min at 37 °C. At the indicated time points, cells were labeled with anti-dsRNA mAb (*black lines*) or mouse IgG2a (*shaded histogram*) and FITC-labeled secondary Ab. The cells were analyzed on a FACS Calibur. AQ: J

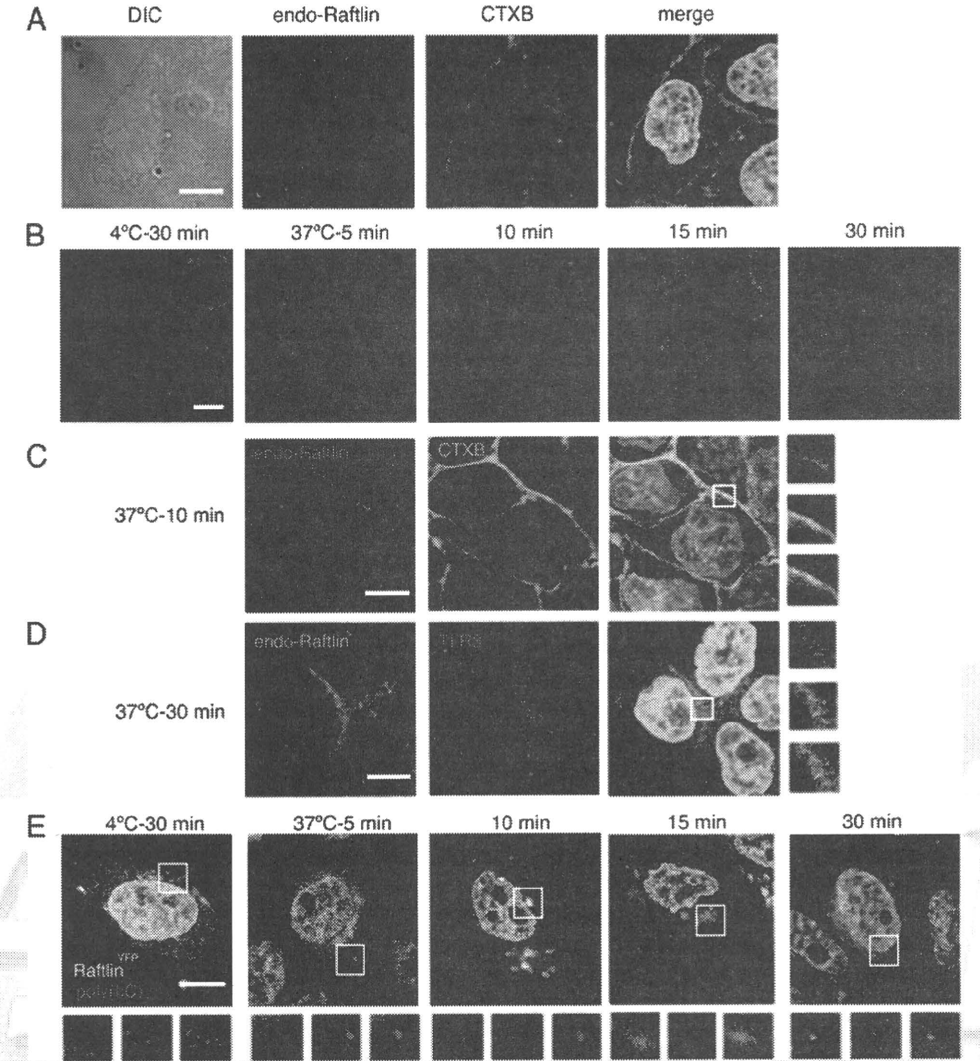

COLOR

FIGURE 4. **Translocation of Raftlin in response to poly(I:C).** *A*, confocal images of endogenous Raftlin in HeLa cells. Fixed and permeabilized cells were stained with anti-Raftlin pAb and Alexa Fluor 488/CTXB. *Red*, endogenous Raftlin; *green*, CTXB; *blue*, nuclei with DAPI. *Bar*, 10 μm. *B–D*, spatiotemporal mobilization of endogenous Raftlin in response to poly(I:C). HeLa cells were incubated with 40 μg/ml of poly(I:C) as described in the legend to Fig. 3. At the indicated periods, cells were fixed and stained with anti-Raftlin pAb (*B*), anti-Raftlin pAb and Alexa Fluor 488/CTXB (*C*), or anti-Raftlin pAb and anti-TLR3 mAb (*D*). Representative data from the indicated time points are shown. *B* and *C*, *red*, endogenous Raftlin; *green*, Alexa 488/CTXB. *D*, *green*, endogenous Raftlin; red, TLR3; *blue*, nuclei with DAPI. *Bar*, 10 μm. *E*, association of Raftlin with poly(I:C). Confocal images of poly(I:C) uptake by HeLa cells expressing Raftlin^{YFP}. HeLa cells were transfected with Raftlin^{YFP} and incubated with 40 μg/ml of Texas Red/poly(I:C) as described above. At the indicated periods, cells were fixed and visualized by confocal microscopy. *Lower panels* show ×2 magnified images of the *insets* in the *upper panels*. *Yellow*, Raftlin^{YFP}; *red*, Texas Red/poly(I:C); *blue*, nuclei with DAPI. *Bar*, 10 μm.

(K1) or mouse IgG2a as a control (1 μg) in the presence of human IgG (10 μg) for 30 min at 4 °C in FACS buffer (Dulbecco's phosphate-buffered saline containing 0.5% BSA and 0.1% sodium azide) and then incubated with FITC-labeled secondary Ab. Cells were analyzed on a FACS Calibur flow cytometer (BD Biosciences).

Statistical Analysis—Statistical significance of differences between groups was determined by the Student's *t* test.

RESULTS

Raftlin Participates in Poly(I:C)-induced TLR3-mediated Signaling—We previously demonstrated that poly(I:C) binds to human MoDCs and HEK293 cells (27). Because poly(I:C) also activates B cells (32), we screened B cell lines capable of binding poly(I:C) and found that Raji cells bound poly(I:C) at an equivalent level to MoDCs (supplemental Fig. S1). To identify the proteins involved in poly(I:C) cellular uptake, we isolated the poly(I:C)-binding proteins from Raji cell lysates by sequential affinity chromatography using Sepharose, poly(U)-Sepharose, and poly(I:C)-Sepharose. The eluate from poly(U)- or poly(I:C)-Sepharose was subjected to SDS-PAGE, followed by mass spectrometric analyses. A total of 127 proteins were identified, which preferentially bound to poly(I:C)-Sepharose rather than to poly(U)-Sepharose (supplemental Table S2). They included several proteins with a dsRNA-binding motif, such as interferon-induced dsRNA-activated protein kinase (supplemental Table 3). Also, clathrin heavy chain 1 and several cytoskeleton molecules, such as tubulin and actinin-1, were identified, suggesting that poly(I:C) uptake machinery might be isolated from the cell lysates as a complex. In the membrane/cytoskeleton group, only four are membrane-associated proteins (supplemental Table S3). We selected transmembrane proteins LYRIC

AQ: G ZSI ZSI ZSI ZSI

(also called Astrocyte elevated gene 1) and 4F2 cell surface antigen heavy chain (4F2, also named CD98), and a cytoplasmic protein Raftlin that contains a membrane-anchoring motif at the N terminus. Because HEK293 cells express these molecules, we first examined whether they are involved in poly(I:C)-induced TLR3-mediated signaling by gene silencing. As a positive control, knockdown of TICAM-1 was performed. Interestingly, poly(I:C)-induced TLR3-mediated IFN-β promoter activation was greatly reduced when Raftlin was knocked down in HEK293 cells, whereas silencing of the LYRIC or 4F2 genes did
F1 not affect poly(I:C) function (Fig. 1*A*, *left-hand panel*). Poly(I:C)-induced TLR3-mediated NF-κB activation was also decreased in Raftlin knockdown HEK293 cells, in a similar way to TICAM-1 knockdown cells (Fig. 1*B*). In contrast, TLR2-mediated NF-κB activation was substantially induced in all cells subjected to gene silencing (Fig. 1*C*). The failure of IFN-β promoter activation in Raftlin knockdown HEK293 cells was also observed when cells were stimulated with increasing amounts of poly(I:C) (Fig. 1*D*). These results strongly suggest that Raftlin participates in poly(I:C)-induced TLR3 activation.

Raftlin Is Essential for Poly(I:C)-induced IFN-β Production in HeLa Cells—Raftlin was originally identified as a major lipid raft protein required for lipid raft integrity, B cell receptor signal transduction, and modulation of T cell receptor signaling (29, 33). We analyzed the expression of Raftlin and Raftlin-2, a homologue of Raftlin, in HEK293, HeLa, and Raji cells by RT-
F2 PCR. As shown in Fig. 2*A*, these cell lines express Raftlin but not Raftlin-2 mRNA. The protein expression level of Raftlin was further examined by immunoblotting with an anti-human Raftlin pAb (29). Raftlin was abundantly expressed in Raji cells, and expressed at lower levels in HEK293 and HeLa cells (Fig. 2*B*). Poly(I:C)-induced IFN-β mRNA expression was greatly diminished by knockdown of Raftlin in HeLa cells, in a similar way to TICAM-1 knockdown. In contrast, HeLa cells transfected with siRNA for 4F2 or LYRIC efficiently responded to
ZSI poly(I:C) (Fig. 2*C*, *left-hand panel*, and supplemental Fig. S2). The expression of TLR3, TICAM-1, MDA5, and IPS-1 was not affected by knockdown of Raftlin (Fig. 2*D*). Thus, Raftlin plays a critical role in poly(I:C)-induced IFN-β production.

Raftlin Is Indispensable for Poly(I:C) Cellular Uptake—To examine the role of Raftlin in poly(I:C)-induced cellular responses, we analyzed cell entry of poly(I:C) in Raftlin knockdown HeLa cells. Texas Red-labeled poly(I:C), whose biological
ZSI activity was similar to that of unlabeled poly(I:C) (supplemental Fig. S3), unevenly bound to the cell surface of HeLa cells either transfected with control siRNA or Raftlin siRNA after 30 min
F3 incubation at 4 °C (Fig. 3*A*, *left panels*). When the incubation condition was changed to 37 °C for 5 min, poly(I:C) was detected as speckles at the cell surface in both cells, although some of the poly(I:C) was internalized in control cells (*second set of panels*). However, after 15 min, poly(I:C) localized diffusely in the endosomal compartments in control cells, whereas it still resided on the cell surface as speckles in Raftlin knockdown cells (*third set of panels*). Thus, clustering of the uptake receptor occurs without internalization in Raftlin knockdown cells. After 30 min, poly(I:C) accumulated in the endosomal compartments in control cells, where it colocalized with TLR3 (Fig. 3*A*, *upper right panel*). In contrast, Raftlin knockdown

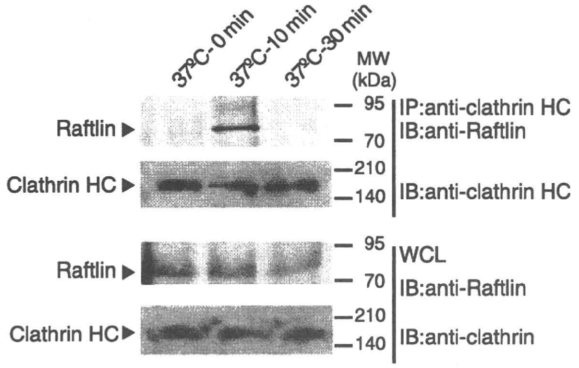

FIGURE 5. **Raftlin associates with clathrin in response to poly(I:C).** HeLa cells were stimulated with 40 μg/ml of poly(I:C) for 0–30 min at 37 °C. At timed intervals, cells were lysed in lysis buffer and clathrin was immunoprecipitated (*IP*) using an anti-clathrin heavy chain (*HC*) mAb. The immunoprecipitants were resolved on SDS-PAGE (10% gel) under reducing conditions followed by immunoblotting (*IB*) with anti-Raftlin pAb or anti-clathrin HC mAb. Whole cell lysates (*WCL*) were subjected to immunoblotting with anti-Raftlin pAb or anti-clathrin HC mAb to detect endogenous protein expression. Molecular mass markers are indicated on the *right*.

HeLa cells did not permit cell entry of poly(I:C). Consistent with these results, flow cytometric analysis showed that surface poly(I:C) disappeared in control but not in Raftlin knockdown HeLa cells (Fig. 3*B*). After a 30-min incubation at 37 °C, poly(I:C) was detected on the cell surface of ~80% of HeLa cells transfected with Raftlin-siRNA, which reflects the knockdown efficiency.

Because poly(I:C) is internalized into cells by the clathrin-dependent endocytic pathway, we examined whether uptake of transferrin, which occurs in a clathrin-dependent manner, is suppressed by Raftlin knockdown. As shown in Fig. 3*C*, transferrin was internalized into HeLa cells irrespective of Raftlin knockdown. We previously reported that B- and C-type ODNs share their uptake receptor with poly(I:C) in HEK293 cells and MoDCs and are delivered to TLR3-positive endosomes in MoDCs (27). Indeed, FITC-labeled B-type ODN (ODN 2006) failed to enter cells when Raftlin was silenced in HEK293 cells (Fig. 3*D*). These results indicate that Raftlin is essential for uptake of poly(I:C) and B- and C-type ODNs via receptor-mediated endocytosis.

Raftlin Is Involved in the Uptake Machinery for Poly(I:C)—A previous study showed that Raftlin is localized exclusively in lipid rafts by fatty acylation of the N-terminal Gly-2 and Cys-3 residues in human B cells (29). We analyzed the subcellular localization of Raftlin in HeLa cells. Endogenous Raftlin was localized diffusely in the cytoplasm and did not merge with CTXB, which binds to the lipid raft molecule GM1, suggesting the cell type-dependent localization of Raftlin (Fig. 4*A*). We F4
next examined the translocation of Raftlin in response to poly(I:C). At the poly(I:C) binding step (4 °C, 30 min), Raftlin resided in the cytoplasm (Fig. 4*B*, *left panel*). After a 5-min incubation at 37 °C, most of the Raftlin remained localized in the cytoplasm. However, after 10 min, membrane-associated Raftlin was observed, which partially colocalized with CTXB (Fig. 4, *B*, *third panel*, and *C*). Interestingly, Raftlin transferred to the endosomal structures from the plasma membrane within 15 min, and colocalized with TLR3 after 30 min of incubation (Fig. 4*D*).

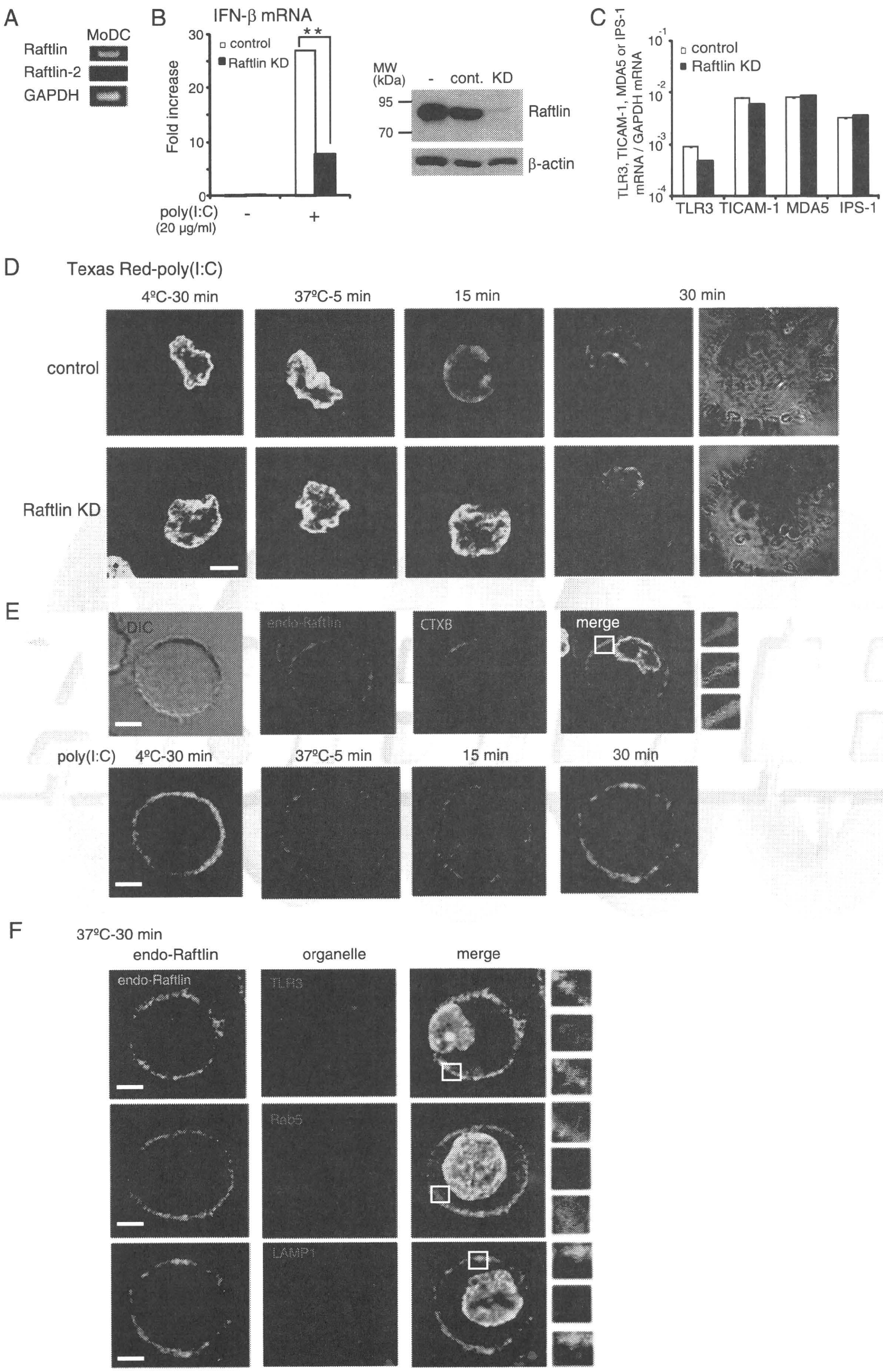
A
MoDC
Raftlin
Raftlin-2
GAPDH
B
IFN-β mRNA
control
Raftlin KD
**
Fold increase
30
20
10
0
poly(I:C)
(20 μg/ml)
-
+
MW
(kDa)
-
cont.
KD
95
70
Raftlin
β-actin
C
control
Raftlin KD
TLR3, TICAM-1, MDA5 or IPS-1 mRNA / GAPDH mRNA
TLR3
TICAM-1
MDA5
IPS-1
D
Texas Red-poly(I:C)
4ºC-30 min
37ºC-5 min
15 min
30 min
control
Raftlin KD
E
DIC
endo-Raftlin
CTXB
merge
poly(I:C)
4ºC-30 min
37ºC-5 min
15 min
30 min
F
37ºC-30 min
endo-Raftlin
organelle
merge
TLR3
Rab5
LAMP1

COLOR

Essential Role of Raftlin in Poly(I:C) Cellular Uptake

To visualize the spatiotemporal mobilization of Raftlin and poly(I:C), HeLa cells were transfected with the expression vector for Raftlin^{YFP} and incubated with Texas Red-labeled poly(I:C). The subcellular localization and translocation of Raftlin^{YFP} in response to poly(I:C) were almost similar to those observed with endogenous Raftlin (Fig. 4*E*). Notably, Raftlin^{YFP} co-localized with Texas Red-poly(I:C) at the plasma membrane after 10-min incubation at 37 °C. Thereafter, poly(I:C) was internalized, spread to the endosomal compartments, and then accumulated in the organelles as shown in Fig. 3*A*. A membrane-associated Raftlin^{YFP} appeared to move along with internalized poly(I:C) (Fig. 4*E*).

To clarify the function of Raftlin in poly(I:C) internalization mediated by clathrin, we examined physical association of
F5 Raftlin with clathrin. As shown in Fig. 5, Raftlin did not interact with clathrin in unstimulated HeLa cells. When cells were stimulated with poly(I:C), Raftlin was co-immunoprecipitated with clathrin after a 10-min stimulation. However, after 30 min, Raftlin did not interact with clathrin any more. These results suggest that after poly(I:C) binding to the uptake receptor, Raftlin was recruited to the plasma membrane and associates with the clathrin complex to modulate cargo sorting and delivery.

Raftlin Is Critical for Poly(I:C)-induced IFN-β Production in Human Myeloid DCs—Human MoDCs expressed Raftlin but
F6 not Raftlin-2 mRNA (Fig. 6*A*). When DCs were electrically transfected with siRNA for Raftlin, Raftlin expression was decreased compared with cells transfected with control siRNA (Fig. 6*B*, *right-hand panel*). Poly(I:C)-induced IFN-β mRNA expression was diminished in the Raftlin knockdown DCs (Fig. 6*B*, *left-hand panel*). The mRNA expression levels of TICAM-1, MDA5, and IPS-1 in Raftlin knockdown DCs were comparable with those in control DCs, although TLR3 expression was slightly reduced compared with control cells (Fig. 6*C*). Again, entry of poly(I:C) into Raftlin knockdown DCs was inhibited (Fig. 6*D*).

Raftlin was localized to both the plasma membrane and the cytoplasm of DCs (Fig. 6*E*, *upper panels*). Although membrane-associated Raftlin partially colocalized with CTXB, lipid raft disruption with MβCD in DCs did not affect poly(I:C) cellular
ZSI uptake (supplemental Fig. S4). The mobilization of Raftlin in response to poly(I:C) was similar to that observed in HeLa cells (Fig. 6*E*, *lower panels*). After 30 min, Raftlin colocalized with TLR3 and Rab5 but not with LAMP1, indicating that Raftlin, together with the poly(I:C) uptake receptor, moves from the plasma membrane to the TLR3-positive early endosomes (Fig. 6*F*).

To determine the physiological function of Raftlin, we analyzed poly(I:C)-induced IFN-β production by BMDCs from wild-type or Raftlin$^{-/-}$ mice. Remarkably, wild-type and Raftlin$^{-/-}$ BMDCs expressed mouse Raftlin-2 mRNA at equivalent levels (Fig. 7*A*). There was no significant difference in F7
poly(I:C)-induced IFN-β production between wild-type and Raftlin$^{-/-}$ BMDCs (Fig. 7*B*). In addition, cellular uptake of poly(I:C) in Raftlin$^{-/-}$ BMDCs was comparable with that in wild-type BMDCs (Fig. 7*C*). To test the possibility that the Raftlin function is compensated with Raftlin-2 in Raftlin$^{-/-}$ BMDCs as observed in B cell receptor signaling in Raftlin$^{-/-}$ mouse B cells (33), we knocked down of mouse Raftlin-2 in Raftlin$^{-/-}$ BMDCs by infection with Raftlin-2 shRNA-expressing lentiviral particles and analyzed the cellular response to poly(I:C). Mouse Raftlin-2 expression was partially decreased in Raftlin$^{-/-}$ BMDCs (Fig. 7*D*, *right-hand panel*). Poly(I:C)-induced IFN-β mRNA expression was partially but significantly decreased in Raftlin-2 knockdown Raftlin$^{-/-}$ BMDCs (Fig. 7*D*, *left-hand panel*). Furthermore, internalization of Texas Red-labeled poly(I:C) was inhibited in ~40% of Raftlin$^{-/-}$ BMDCs infected with mouse Raftlin-2 shRNA lentiviral particles, reflecting the knockdown efficiency of mouse Raftlin-2 (Fig. 7*E*). These results suggest that mouse Raftlin-2 participates in poly(I:C) cellular uptake in Raftlin$^{-/-}$ BMDCs.

DISCUSSION

Recent studies using mouse implanted tumor models indicate that poly(I:C) is a promising adjuvant for tumor vaccines because it promotes adaptive anti-tumor responses through the activation of myeloid DCs and induction of type I IFN production by multiple type of cells (10–15). However, it remains unresolved how poly(I:C) is delivered from the extracellular fluid to the intracellular poly(I:C) sensors localized on the endosomal membrane or cytoplasm.

In this study, we demonstrated that Raftlin is essential for poly(I:C)-induced cellular responses in human myeloid DCs and epithelial cells by mediating the cellular uptake of poly(I:C). Raftlin was originally identified as a major raft protein in B cells that co-localized with B cell receptor in the lipid raft before and after B cell receptor stimulation (29). However, subcellular localization of endogenous Raftlin appears to depend on the cell types. We found that in unstimulated HeLa cells, endogenous Raftlin localized diffusely in the cytoplasm and did not co-

FIGURE 6. **Raftlin is critical for poly(I:C)-induced IFN-β production in human myeloid DCs.** *A*, MoDCs express Raftlin but not Raftlin-2 mRNA. *B*, poly(I:C)-induced IFN-β production was decreased in Raftlin knockdown DCs (*left-hand panel*). Control and Raftlin knockdown DCs in a 24-well plate (7 × 10^5/ml) were stimulated with 20 μg/ml of polymyxin B-treated poly(I:C) for 4 h. Total RNA was extracted and subjected to RT qPCR analysis for the expression of IFN-β. Data are representative of three separate experiments with similar results (mean ± S.D.). **, $p < 0.01$. Protein expression of Raftlin in DCs (4 × 10^5) before and after siRNA transfection is shown (*B*, *right panel*). *C*, expression of TLR3, TICAM-1, MDA5, and IPS-1 in DCs. Total RNA from control and Raftlin knockdown DCs were extracted and subjected to RT-qPCR analysis for the expression of mRNA. Expression of each gene was normalized to GAPDH mRNA expression. *D*, uptake of Texas Red/poly(I:C) by MoDCs transfected with control siRNA (*upper panels*) or siRNA for Raftlin (*lower panels*). Control or Raftlin knockdown DCs were incubated with 40 μg/ml of Texas Red/poly(I:C) for 30 min at 4 °C. After washing, cells were incubated for up to 30 min at 37 °C. At the indicated periods, cells were fixed and visualized by confocal microscopy. Representative images from 20 fields in the indicated time points are shown. *Red*, Texas Red/poly(I:C); *blue*, nuclei with DAPI. *Bar*, 5 μm. *E* and *F*, confocal images of endogenous Raftlin in MoDCs in response to poly(I:C). *E*, *upper panels*, DCs were fixed and stained with anti-Raftlin pAb and Alexa 488/CTXB. *Red*, endogenous Raftlin; *green*, Alexa 488/CTXB; *blue*, nuclei with DAPI. *E*, *lower panels*, and *F*, DCs were incubated with 40 μg/ml of poly(I:C) as described in the legend to Fig. 4. At the indicated periods, cells were fixed and stained with anti-Raftlin pAb, anti-TLR3 mAb, anti-Rab5 mAb, or anti-LAMP1 mAb and Alexa Fluor-conjugated secondary Abs. Representative data from the indicated time points are shown. *Green*, endogenous Raftlin; *red*, TLR3, Rab5, or LAMP-1; *blue*, nuclei with DAPI. *Bar*, 5 μm.

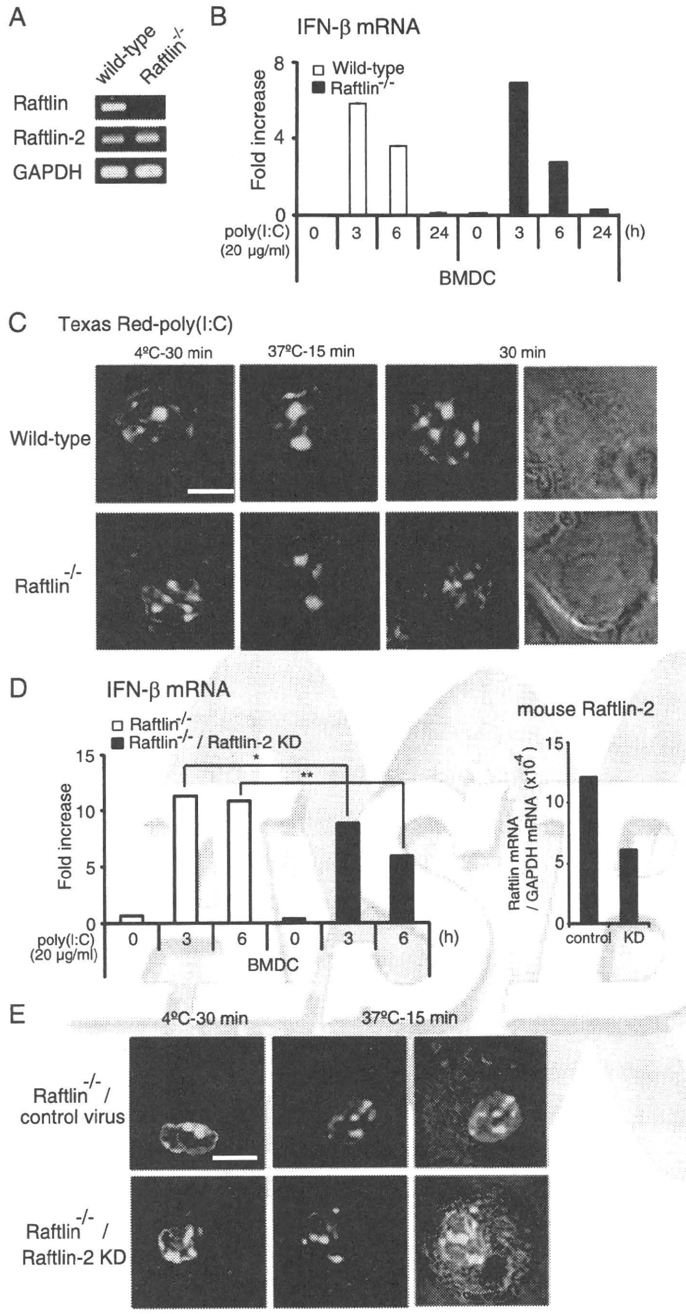

FIGURE 7. **Poly(I:C) uptake and IFN-β production by Raftlin$^{-/-}$ BMDCs.** *A*, expression of Raftlin and Raftlin-2 mRNAs in BMDCs from wild-type or Raftlin$^{-/-}$ mice. *B*, IFN-β mRNA expression in BMDCs from wild-type or Raftlin$^{-/-}$ mice in response to poly(I:C). Cells were stimulated with 20 μg/ml of polymyxin B-treated poly(I:C). At the indicated time points, cells were washed and total RNA was extracted. RT qPCR was performed using the primers for mouse IFN-β. Data (mean $\pm$ S.D.) are representative of three separate experiments with similar results. *C*, BMDCs from wild-type (*upper panels*) or Raftlin$^{-/-}$ mice (*lower panels*) were incubated with 40 μg/ml of Texas Red/poly(I:C) for 30 min at 4 °C. After washing, cells were incubated for up to 30 min at 37 °C. At timed intervals, cells were fixed and visualized by confocal microscopy. Representative images from 20 fields in the indicated time points are shown. *Red*, Texas Red/poly(I:C); *blue*, nuclei with DAPI. *Bar*, 5 μm. *D*, poly(I:C)-induced IFN-β mRNA expression in control and Raftlin-2 knockdown Raftlin$^{-/-}$ BMDCs. *Left-hand panel*, control and Raftlin-2 knockdown Raftlin$^{-/-}$ BMDCs were stimulated with 20 μg/ml of polymyxin B-treated poly(I:C). At the indicated time points, IFN-β mRNA expression was analyzed as described above. *Right-hand panel*, mouse Raftlin-2 mRNA expression. Representative data from two independent experiments are shown. *, $p < 0.05$; **, $p < 0.01$. *E*, poly(I:C) cellular uptake by control and Raftlin-2 knockdown Raftlin$^{-/-}$ BMDCs. Representative images from 20 fields in the indicated time points are shown. In Raftlin$^{-/-}$ BMDCs infected with mouse Raftlin-2 shRNA lentiviral particles, 40% of cells fail to internalize poly(I:C) after a 15-min incubation at 37 °C. The number of cells lacking Texas Red/poly(I:C) internalization/total number of cells were for control Raftlin$^{-/-}$ BMDCs, 0/137, and Raftlin-2 knockdown Raftlin$^{-/-}$ BMDCs, 106/260. *Red*, Texas Red/poly(I:C); *blue*, nuclei with DAPI. *Bar*, 5 μm.

ZSI

COLOR

localize with CTXB (Fig. 4), whereas in MoDCs it localized to both the plasma membrane and the cytoplasm and membrane-associated Raftlin partially merged with CTXB (Fig. 6*E*). In these cells, poly(I:C) stimulation induced the translocation of Raftlin from the cytoplasm to the plasma membrane where it cooperated with uptake receptor to deliver poly(I:C) to TLR3-positive endosomes (Figs. 4 and 6*F*). Thus, Raftlin is involved in the nucleocapture complex triggering poly(I:C)-mediated TLR3 activation, and appears to act downstream of immune receptors in a cell type-specific manner.

Notably, Raftlin$^{-/-}$ BMDCs that express Raftlin-2 normally took up poly(I:C) (Fig. 7*C*). The expression of Raftlin or Raftlin-2 depends on the cell type. Mouse Raftlin-2 is expressed in B cells but not T cells and is thought to function in a similar way to Raftlin in mouse B cells (33). Because poly(I:C)-induced IFN-β mRNA expression and internalization of poly(I:C) were decreased when mouse Raftlin-2 was knocked down in Raftlin$^{-/-}$ BMDCs (Fig. 7, *D* and *E*), mouse Raftlin-2 participates in poly(I:C) uptake in Raftlin$^{-/-}$ BMDCs. In humans, MoDCs, HEK293 cells, and HeLa cells did not express Raftlin-2 mRNA. Hence, human Raftlin plays a key role in poly(I:C)-induced cellular responses in the absence of Raftlin-2.

The molecular mechanism by which Raftlin cooperates with the uptake receptor to mediate cell entry of poly(I:C) and B- and C-type ODNs is currently unknown. As shown in Fig. 3*A*, clustering of the uptake receptor occurs without internalization in the absence of Raftlin. Because disruption of the lipid raft by treatment with MβCD did not affect internalization of poly(I:C) (supplemental Fig. S4), Raftlin may participate in the assembly of the uptake machinery for poly(I:C) and B- and C-type ODNs independently of lipid raft function. We have previously demonstrated that poly(I:C) is internalized via the clathrin-mediated endocytosis (27). Indeed, Raftlin associated with clathrin after poly(I:C) stimulation (Fig. 5). Thus, Raftlin might be involved in the clathrin and clathrin-associated adapter protein complexes at the plasma membrane and participates in cargo sorting and delivery to the TLR3-positive endosome (34).

Intriguingly, A-type ODN that activates plasmacytoid DCs to induce IFN-α was unable to bind to myeloid DCs (27). A-type ODN binds to high mobility group box 1 and augments the binding of high mobility group box 1 to receptor for advanced glycation end products (35). A-type ODN-high mobility group box 1 complex enhances TLR9-mediated IFN-α production by plasmacytoid DCs in a receptor for advanced glycation end product-dependent manner, although receptor for advanced glycation end products is not essential for internalization of A-type ODN or A-type ODN-high mobility group box 1 complexes. An unidentified uptake receptor for A-type ODN must reside on plasmacytoid DCs. Although whether Raftlin participates in the uptake of A-type ODN in human plasmacytoid DCs remains to be examined, we surmise that exogenous nucleic acids are recognized by cell surface receptors that form distinct nucleocapture complexes to deliver nucleic acids to intracellular organelles.

The adjuvant activity of poly(I:C) is derived from the activation of two innate immune sensors, TLR3 and MDA5, in myeloid DCs. No RNA molecule has been reported besides poly(I:C) that extracellulary activates either TLR3 or MDA5. Identification of the uptake receptor for poly(I:C) in DCs is important to elucidate the mechanism by which poly(I:C) is localized to TLR3 and MDA5, as well as to develop a poly(I:C)-related adjuvant that is selectively transferred to TLR3 and/or MDA5.

Acknowledgments—We thank Dr. Y. Miyamoto and K. Shida (Osaka Medical Center for Cancer, Osaka, Japan) for technical support and Drs. H. Oshiumi, T. Ebihara, H. Takaki, H. H. Aly, and J. Kasamatsu for invaluable discussions. We also thank Dr. J. P. Atkinson (Washington University) for reviewing this manuscript.

REFERENCES

AQ: H
1. Nagano, Y., and Kojima, Y. (1954) *C.R. Seans. Soc. Biol. Fil.* **148,** 1700–1702
2. Lindenmann, J., Burke, D. C., and Isaacs, A. (1957) *Br. J. Exp. Pathol.* **38,** 551–562
3. Field, A. K., Tytell, A. A., Lampson, G. P., and Hilleman, M. R. (1967) *Proc. Natl. Acad. Sci. U.S.A.* **58,** 1004–1010
4. Alexopoulou, L., Holt, A. C., Medzhitov, R., and Flavell, R. A. (2001) *Nature* **413,** 732–738
5. Matsumoto, M., Kikkawa, S., Kohase, M., Miyake, K., and Seya, T. (2002) *Biochem. Biophys. Res. Commun.* **293,** 1364–1369
6. Yoneyama, M., Kikuchi, M., Matsumoto, K., Imaizumi, T., Miyagishi, M., Taira, K., Foy, E., Loo, Y. M., Gale, M., Jr., Akira, S., Yonehara, S., Kato, A., and Fujita, T. (2005) *J. Immunol.* **175,** 2851–2858
7. Kato, H., Takeuchi, O., Sato, S., Yoneyama, M., Yamamoto, M., Matsui, K., Uematsu, S., Jung, A., Kawai, T., Ishii, K. J., Yamaguchi, O., Otsu, K., Tsujimura, T., Koh, C. S., Reis e Sousa, C., Matsuura, Y., Fujita, T., and Akira, S. (2006) *Nature* **441,** 101–105
8. Gitlin, L., Barchet, W., Gilfillan, S., Cella, M., Beutler, B., Flavell, R. A., Diamond, M. S., and Colonna, M. (2006) *Proc. Natl. Acad. Sci. U.S.A.* **103,** 8459–8464
9. Schultz, O., Diebold, S. S., Chen, M., Näslund, T. I., Nolte, M. A., Alexopoulou, L., Azuma, Y. T., Flavell, R. A., Liljeström, P., and Reis e Sousa, C. (2005) *Nature* **433,** 887–892
10. Matsumoto, M., and Seya, T. (2008) *Adv. Drug Deliv. Rev.* **60,** 805–812
11. Kumar, H., Koyama, S., Ishii, K. J., Kawai, T., and Akira, S. (2008) *J. Immunol.* **180,** 683–687
12. McCartney, S., Vermi, W., Gilfillan, S., Cella, M., Murphy, T. L., Schreiber, R. D., Murphy, K. M., and Colonna, M. (2009) *J. Exp. Med.* **206,** 2967–2976
13. Miyake, T., Kumagai, Y., Kato, H., Guo, Z., Matsushita, K., Satoh, T., Kawagoe, T., Kumar, H., Jang, M. H., Kawai, T., Tani, T., Takeuchi, O., and Akira, S. (2009) *J. Immunol.* **183,** 2522–2528
14. Longhi, M. P., Trumpfheller, C., Idoyaga, J., Caskey, M., Matos, I., Kluger, C., Salazar, A. M., Colonna, M., and Steinman, R. M. (2009) *J. Exp. Med.* **206,** 1589–1602
15. Ebihara, T., Azuma, M., Oshiumi, H., Kasamatsu, J., Iwabuchi, K., Matsumoto, K., Saito, H., Taniguchi, T., Matsumoto, M., and Seya, T. (2010) *J. Exp. Med.* **27,** 2675–2687 AQ: I
16. Matsumoto, M., Funami, K., Tanabe, M., Oshiumi, H., Shingai, M., Seto, Y., Yamamoto, A., and Seya, T. (2003) *J. Immunol.* **171,** 3154–3162
17. Funami, K., Sasai, M., Ohba, Y., Oshiumi, H., Seya, T., and Matsumoto, M. (2007) *J. Immunol.* **179,** 6867–6872
18. Oshiumi, H., Matsumoto, M., Funami, K., Akazawa, T., and Seya, T. (2003) *Nat. Immunol.* **4,** 161–167
19. Yamamoto, M., Sato, S., Hemmi, H., Hoshino, K., Kaisho, T., Sanjo, H., Takeuchi, O., Sugiyama, M., Okabe, M., Takeda, K., and Akira, S. (2003) *Science* **301,** 640–643
20. Kawai, T., Takahashi, K., Sato, S., Coban, C., Kumar, H., Kato, H., Ishii, K. J., Takeuchi, O., and Akira, S. (2005) *Nat. Immunol.* **6,** 981–988
21. Seth, R. B., Sun, L., Ea, C. K., and Chen, Z. J. (2005) *Cell* **122,** 669–682
22. Meylan, E., Curran, J., Hofmann, K., Moradpour, D., Binder, M., Bartenschlager, R., and Tschopp, J. (2005) *Nature* **437,** 1167–1172
23. Xu, L. G., Wang, Y. Y., Han, K. J., Li, L. Y., Zhai, Z., and Shu, H. B. (2005) *Mol. Cell* **19,** 727–740
24. Lee, H. K., Dunzendorfer, S., Soldau, K., and Tobias, P. S. (2006) *Immunity* **24,** 153–163
25. Limmon, G. V., Arredouani, M., McCann, K. L., Corn Minor, R. A., Kobzik, L., and Imani, F. (2008) *FASEB J.* **22,** 159–167
26. Krieg, A. M. (2002) *Annu. Rev. Immunol.* **20,** 709–760
27. Itoh, K., Watanabe, A., Funami, K., Seya, T., and Matsumoto, M. (2008) *J. Immunol.* **181,** 5522–5529
28. Ranjith-Kumar, C. T., Duffy, K. E., Jordan, J. L., Eaton-Bassiri, A., Vaughan, R., Hoose, S. A., Lamb, R. J., Sarisky, R. T., and Kao, C. C. (2008) *Mol. Cell. Biol.* **28,** 4507–4519
29. Saeki, K., Miura, Y., Aki, D., Kurosaki, T., and Yoshimura, A. (2003) *EMBO J.* **22,** 3015–3026
30. Obuse, C., Iwasaki, O., Kiyomitsu, T., Goshima, G., Toyoda, Y., and Yanagida, M. (2004) *Nat. Cell Biol.* **6,** 1135–1141
31. Ebihara, T., Shingai, M., Matsumoto, M., Wakita, T., and Seya, T. (2008) *Hepatology* **48,** 48–58
32. Ding, C., Wang, L., Al-Ghawi, H., Marroquin, J., Mamula, M., and Yan, J. (2006) *Eur. J. Immunol.* **36,** 2013–2024
33. Saeki, K., Fukuyama, S., Ayada, T., Nakaya, M., Aki, D., Takaesu, G., Hanada, T., Matsumura, Y., Kobayashi, T., Nakagawa, R., and Yoshimura, A. (2009) *J. Immunol.* **182,** 5929–5937
34. Ohno H. (2006) *J. Cell Sci.* **119,** 3719–3721
35. Tian, J., Avalos, A. M., Mao, S. Y., Chen, B., Senthil, K., Wu, H., Parroche, P., Drabic, S., Golenbock, D., Sirois, C., Hua, J., An, L. L., Audoly, L., La Rosa, G., Bierhaus, A., Naworth, P., Marshak-Rothstein, A., Crow, M. K., Fitzgerald, K. A., Latz, E., Kiener, P. A., and Coyle, A. J. (2007) *Nat. Immunol.* **8,** 487–496

Vaccine 28S (2010) B75–B77

Contents lists available at ScienceDirect

Vaccine

journal homepage: www.elsevier.com/locate/vaccine

Review

Establishment of specific pathogen-free macaque colonies in Tsukuba Primate Research Center of Japan for AIDS research

Yasuhiro Yasutomi [a,b,*]

[a] Laboratory of Immunoregulation and Vaccine Research, Tsukuba Primate Research Center, National Institute of Biomedical Innovation, Tsukuba, Ibaraki 305-0843, Japan
[b] Department of Immunoregulation, Mie University Graduate School of Medicine, Mie 514-8507, Japan

ARTICLE INFO

Article history:
Received 9 April 2009
Received in revised form 13 August 2009
Accepted 18 September 2009

Keywords:
Macaque
SPF
Virus

ABSTRACT

Cynomolgus monkeys have been maintained in indoor facilities as closed colony monkeys in Tsukuba Primate Research Center in Japan since 1978. Several microorganisms, including bacteria, parasites and viruses, were eliminated from the cynomolgus monkeys in this colony of TPRC. Various kinds of viruses (B virus, measles virus, simian varicella virus, simian immunodeficiency virus, simian T cell leukemia virus, simian D type retrovirus, simian cytomegalovirus, simian Epstein-Barr virus, and simian foamy virus), bacteria (*Shigella, Salmonella* and *Mycobacteria spp.*) and intestinal helminth were chosen as target microorganisms to establish a specific pathogen-free (SPF) colony. Except for a few pathogens (simian D type retrovirus, simian Epstein-Barr virus, and simian foamy virus), selected pathogens were completely eliminated from all monkeys in TPRC. In this review, the history of establishment of SPF cynomolgus monkey colonies in Japan is described.

Contents

1. Introduction

Nonhuman primates are critical resources for biomedical research. Macaque monkeys are one of the key nonhuman primate models that share nearly all characteristics with humans. Conditions of experimental animals are very important for biomedical experiments. The animals should not be infected with microorganisms because microorganism infection may affect results. Moreover, some pathogens are likely to harm not only monkeys but also humans in experiments involving macaques. For these reasons, there is a need for specific pathogen-free (SPF) macaque colonies for research purposes, biohazard avoidance and maintenance of health levels in established colonies (Table 1).

Tsukuba Primate Research Center (TPRC) in Japan has a large-scale breeding colony of experimental cynomolgus monkeys (approximately 1500 monkeys), which play a significant role in the development of pharmaceutical products and medical technologies. The center is the forefront facility in Japan that both supplies laboratory-bred monkeys, mainly cynomolgus monkeys, and performs medical research. Cynomolgus monkeys have been maintained in indoor facilities as closed colony monkeys in TPRC since 1978 [1]. In addition to quality control, supply, research resource development, and basic technology development involving the experimental monkeys, evaluation of state-of-the-art medical technology, evaluation of the efficacy of new drugs and safety assessments are also performed using the monkeys. The establishment of SPF macaques is therefore necessary in TPRC.

* Laboratory of Immunoregulation and Vaccine Research, Tsukuba Primate Research Center, National Institute of Biomedical Innovation, 1-1 Hachimandai, Tsukuba, Ibaraki 305-0843, Japan. Tel.: +81 29 837 2073; fax: +81 29 837 2053.
E-mail addresses: yasutomi@nibio.go.jp, yasutomi@doc.medic.mie-u.ac.jp.

0264-410X/$ – see front matter © 2009 Elsevier Ltd. All rights reserved.
doi:10.1016/j.vaccine.2009.09.079

Table 1
History of establishment of SPF cynomolgus monkeys in TPTC.

Year	Target microorganism	Complete elimination from TPRC
1978–1982	BV, MV, *Shigella*, *Salmonella*, *Mycobacteria*, helminth	MV, *Shigella*, *Salmonella*, *Mycobacteria*,
1983–1994	BV, SVV, SIV, STLV-1, SRV/D helminth	SIV, STLV-1, helminth
1995–2004	BV, SVV, SRV/D,	BV, SVV,
2004–Present	SRV/D (73%)[a], LCV (50%)[a], SFV (31%)[a]	CMV

[a] Infection rate of all cynomolgus monkeys in TPRC at present.

The cynomolgus monkeys in TPRC were obtained from Indonesia, Malaysia and Philippines [1]. The monkeys have been bred as pure blood of each origin without interbreed crossing. These pure blood monkeys should be important for comparison of various genetic effects in biological studies including vaccine development. The establishment of SPF colonies in TPRC is also important for this reason. These three pure blood colonies and one mixed blood colony each consist of approximately 100 SPF cynomolgus monkeys. In this review, attempts to establish SPF macaque colonies for advanced biomedical research are reported.

1.1. First term (1978–1882)

Several kinds of microorganisms were chosen for elimination from colony monkeys. Two viruses (B virus and measles virus), three species of bacteria (*Shigella*, *Salmonella* and *Mycobacteria spp.*) and intestinal helminths were selected as the first target pathogens for elimination in macaque colonies. B virus (BV, *Cercopithecine herpesvirus* 1) is an alphaherpesvirus that naturally infects macaque monkeys. In macaques, the virus typically causes a self-limiting disease similar to herepes simplex virus disease in humans [2]. In surprising contrast, BV infection in humans has resulted in the death of 80% of individuals [2]. Therefore, BV was firstly chosen as an SPF target pathogen for prevention of biohazard risks by this virus. The BV infections were detected by BV-specific antibody (Ab) response in sera using an ELISA system (BioReliance Co., USA). Prevention of the spread of BV in the macaque colony was carried out by early weaning of babies from mothers. Infection of the virus in plasma of the prematurely weaned monkeys was confirmed by a BV-specific Ab several times at intervals of 3–6 months. Measles, caused by measles virus (MV) infection, remains a major cause of infant mortality despite the availability of a safe and effective live attenuated virus vaccine. MV-free cynomolgus monkeys are required, since one of the purposes to supply cynomolgus monkeys in TPRC is certification tests for human measles vaccine. MV infection was examined in all monkeys by detection of specific Ab reaction in sera by ELISA and MV antigen (Ag) detected by RT-PCR. Although most of the cynomolgus monkeys from Asia were infected with MV, asymptomatic monkeys with MV excretion in plasma, urine and other biological fluid were not reproduced in TPRC. The MV-infected monkeys were eliminated by this breeding program. Two species of bacteria, *Salmonella* and *Shigella spp.*, were detected by cultivation of rectal or fecal swab samples. Monkeys having these bacteria received drug treatment (200 mg of sulfamethoxazole and 40 mg of trimethoprim once a day for 3 days by oral administration even to *Salmonella*, 200 mg of fosofomycin once a day for 3 days by oral administration even to *Shigella*) if they showed no clinical symptoms of infection with these bacteria. Infection with *Mycobacteria spp.* responsible for tuberculosis was examined by tuberculin (TB) skin tests, and monkeys with positive results of TB skin tests were eliminated. Infection with MV, *Salmonella*, *Shigella* or *Mycobacteria spp.* has not been detected in any monkeys in TPRC since 1982. Cynomolgus monkeys excreting helminth eggs in feces were given anthelimintics (ivermectin 200 μg/kg s.c twice for 2 weeks interval; metronidazol 40 mg/kg once a day for 5 days by oral administration; thiabendazole 50 mg/kg once a day for 3 days by oral administration and mebendazole 20 mg/kg once a day for 3 days by oral administration).

1.2. Second and third terms (1983–1994)

In addition to targeting BV and helminths for elimination from TPRC, simian immunodeficiency virus (SIV), simian T cell leukemia virus (STLV), simian D type retrovirus (SRV/D) and simian varicella virus (SVV) were newly targeted to establish SPF monkey colonies in 1983–1994. Although an AIDS model induced by SIV is very useful for AIDS studies, SIV is not present in macaques from Asia unless they have been experimentally exposed. In fact, natural infection with SIV was not seen in any of the monkeys in TPRC examined by ELISA for detection of SIV-specific Ab in sera. STLV is widely present in all New and Old World primate species. The incidence of STLV infection in most natural simian populations is 5–40%, but it can be much higher in wild monkeys [3,4]. STLV infection was detected in 11.7% of the monkeys in TPRC by IFA using MT-1 cells [5]. These monkeys were eliminated from TPRC over a period of several years. SVV is an alphaherpesvirus that causes varicella in Old World monkeys and establishes latent infection in ganglionic neurons [6]. Outbreaks in many animal facilities have been reported [7]. An outbreak of SVV infection occurred in TPRC during the period from November 1989 to April 1990. Varicella developed in almost 100 monkeys, and 67% of those monkeys died. The rate of infection with SVV in TPRC was 12.9% in 1990. SVV infection can usually be detected by SVV-specific Abs, even in asymptomatic monkeys, and SVV-infected monkeys were eliminated from TPRC in 2000. Attention must be paid to SRV/D both for its risk to macaque colony health and its negative effects on biomedical research. Monkeys infected with SRV/D eventually show symptoms that might be caused by SRV/D infection, such as diarrhea, weight loss and anemia, due to activation attributable to changing conditions of the individual [8–11]. This virus can be transmitted horizontally, vertically or sexually by symptomatic or asymptomatic animals. Moreover, some SRV/D-infected monkeys can become viremic yet remain Ab-negative, allowing infection to escape detection by routine Ab screening [12]. A new subtype of SRV/D, named SRV/D-T, was detected in the colony in TPRC in 2005 [13]. Certain monkeys were found to have plasma viremia of this subtype and did not develop any specific Abs to SRV/D-T. Cynomolgus monkeys in the colony showing SRV/D-T viremia secreted the virus in saliva, urine and feces, and the viruses secreted from these monkeys were thought to be a potential cause of horizontal infections of SRV/D-T. Moreover, there was a high rate of transmission of SRV/D-T infection between mothers and infants in TPRC. Screening for this virus infection was done by detection of both Ab (Western blot analysis) and virus (RT-PCR) in plasma [14]. STLV was completely eliminated from TPRC during the second and third terms.

1.3. Fourth and fifth terms to present (1995–2009)

Monkey infected with BV and SVV were completely eliminated from TPRC in the late 90s. Three viruses, simian cytomegalovirus (CMV), simian Epstein-Barr virus (EBV, simian lymphocryptoviruses (LCV)) and simian foamy virus (SFV), were added as target viruses in a new plan in 1995 to establish SPF monkey colonies. Simian CMV infections have been reported in various species of monkeys, including macaques [15]. This virus is readily transmitted in oral secretions, breast milk and urine [16], and 3% of adult monkeys in TPRC were infected with the virus. CMV infection was detected by IFA or an ELISA system using CMV Ag. Simian EBV has also been detected in several species of Old World and New World primates [17]. This virus is also readily transmitted, and serological surveys indicated that about 90% of adult cynomolgus monkeys in TPRC were infected. Detection of EBV infection was usually done by using commercial available human IFA kit. Infection with these two viruses, CMV and EBV, in macaques are opportunistic infections. Infection with the other virus, SFV, also does not seem to cause disease in nonhuman primates as natural hosts [18]. Humans can be infected with SFV, although the number of known SFV infection cases in humans is small [19]. SFV infection was detected by IFA using SFV Ag. Monkeys infected with SFV are fraught with hazards to workers in a primate center. The rate of infection with SFV in adult monkeys in TPRC was 80%. Detection of SFV was done by Ab response in sera using ELISA. Prevention of the spread of these three viruses, CMV, LCV and SFV, was performed by artificial nursing with feeding formula for baby monkeys that had been removed from their mothers immediately after birth. CMV infection in monkeys has not been detected in TPRC since 2005.

2. Conclusions

SPF nonhuman primate colonies are required for biomedical research with several beneficial effects such as animal health and occupational safety. High quality of laboratory animals is also required for advanced biomedical studies including vaccine research and development. Infectious agents frequently affect the results of animal experiments. The history of establishment of SPF cynomolgus monkeys in TPRC in Japan for evaluation of state-of-the-art medical technology, evaluation of the efficacy of new drugs and new vaccines, and safety assessments has been described in this review.

Acknowledgements

The author would like to thank all workers in TPRC since 1978 for establishing SPF macaque colonies in Japan.

This study was supported by grants from the Ministry of Health, Labor and Welfare of Japan and the Ministry of Education, Culture, Sports, Science and Technology of Japan.

Conflict of interest statement

The author states that they have no conflict of interest.

References

[1] Honjo S. The Japanese Tsukuba Primate Center for Medical Science (TPC): an outline. J Med Primatol 1985;14:75–89.

[2] Whilley RJ, Hillard J. Cercopithecine herpes virus (B virus). In: Knipe DM, Howley PM, Griffin DE, Lamb RA, Martin MA, Roizman B, et al., editors. Fields virology, vol. 2, 5th ed. Philadelphia, PA: Lippincott Williams & Wilkins; 2007. p. 2889–903.

[3] Richards AL, Girl A, Iskandriatl D, Pamgukas J, Sle A, Rosen L, et al. Simian T lymphotropic virus type I infection among wild-caught Indonesian pig-tailed macaques (*Macaque nemastrina*). J AIDS Hum Retrovirol 1998;19: 542–5.

[4] Schillaci M, Jones-Engel L, Engel G, Paramastri Y, Iskandar E, Willson B, et al. Prevalence of enzootic simian viruses among urban performance monkeys in Indonesia. Trop Med Int Health 2005;10:1305–14.

[5] Hayami M, Komuro A, Nozawa K, Shotake T, Ishikawa K, Yamamoto K, et al. Prevalence of antibody to adult T-cell leukemia virus-associated antigens (ATLA) in Japanese monkeys and other non-human primates. Int J Cancer 1984;33:179–83.

[6] Gray WL, Mullis L, Soike KF. Viral gene expression during acute simian varicella virus infection. J Virol 2002;83:841–6.

[7] Gray WL. Simian varicella: a model for human varicella-zoster virus infections. Rev Med Virol 2004;14:363–81.

[8] Daniel MD, Norval KW, Letvin NL, Hunt RD, Sehgal PK, Desrosiers RC. A new type D retrovirus isolated from macaques with an immunodeficiency syndrome. Science 1984;223:602–5.

[9] Marx PA, Maul DH, Osborn KG, Lerche NW, Moody P, Lowenstine LJ, et al. Simian AIDS: isolation of a type D retrovirus and transmission of the diseases. Science 1984;223:1083–6.

[10] Lerche NW, Osborn KG. Simian retrovirus infections: potential confounding variables in primate toxicology studies. Toxicol Pathol 2003;31(Suppl.):103–10.

[11] Guzman RE, Kerlin RL, Zimmerman TE. Histologic lesions in cynomolgus monkeys (*Macaca fascicularis*) naturally infected with simian retrovirus type D: comparison of seropositive, virus-positive, and uninfected animals. Toxicol Pathol 1999;27:672–7.

[12] Kwng HS, Pederson NC, Lerche NW, Osborn KG, Marx PA, Gardner MB. Viremia, antigenemia and serum antibodies in rhesus macaques infected with simian retrovirus type I1 and their relationship to disease course. Lab Invest 1987;56:591–7.

[13] Hara M, Sata T, Kikuchi T, Nakajima N, Uda A, Fujimoto K, et al. Isolation and characterization of new simian retrovirus type D subtype from monkeys at the Tsukuba Primate Center, Japan. Microbes Infect 2005;7:126–31.

[14] Hara M, Kikuchi T, Ono F, Takano J, Ageyama N, Fujimoto K, et al. Survey of captive cynomolgus macaques colonies for SRV/D infection using polymerase chain reaction assays. Comp Med 2005;55:145–9.

[15] Elkington R, Shouskry NH, Walker S, Crough T, Fazou C, Kaur A, et al. Cross-reactive recognition of human and primate cytomegalovirus sequences by human CD4 cytotoxic T lymphocytes for glycoprotein B and H. Eur J Immunol 2004;34:3216–26.

[16] Barry PA, Loxkridge KM, Salamat S, Tinling SP, Yue Y, Zhou SS, et al. Non-human primate models of intrauterine cytomegalovirus infection. ILAR J 2006;47:49–64.

[17] Cho Y-G, Ramer J, Rivaller P, Quink C, Garber RL, Beler DR, et al. An Epstein-Barr-related herpesvirus from marmoset lymphomas. Proc Natl Acad Sci USA 2001;98:1224–9.

[18] Linial ML. Foamy viruses. In: Knipe DM, Howley PM, Griffin DE, Lamb RA, Martin MA, Roizman B, et al., editors. Fields virology. 5th ed. Philadelphia, PA: Lippincott Williams & Wilkins; 2007. p. 2245–63.

[19] Jones-Engel L, May CC, Engel GA, Steinkraus KA, Schillaci MA, Fuentes A, et al. Diverse contexts of zoonotic transmission of simian foamy viruses in Asia. Emerg Infect Dis 2008;14:1200–8.

Transgenic Res (2010) 19:889–895
DOI 10.1007/s11248-009-9358-9

BRIEF COMMUNICATION

Preferential expression and immunogenicity of HIV-1 Tat fusion protein expressed in tomato plant

Marni E. Cueno · Yurina Hibi · Katsuo Karamatsu · Yasuhiro Yasutomi · Kenichi Imai · Antonio C. Laurena · Takashi Okamoto

Received: 11 June 2009 / Accepted: 26 December 2009 / Published online: 14 January 2010

Abstract HIV-1 Tat plays a major role in viral replication and is essential for AIDS development making it an ideal vaccine target providing that both humoral and cellular immune responses are induced. Plant-based antigen production, due to its cheaper cost, appears ideal for vaccine production. In this study, we created a plant-optimized *tat* and mutant (Cys30Ala/Lys41Ala) *tat* (*mtat*) gene and ligated each into a pBI121 expression vector with a stop codon and a *gusA* gene positioned immediately downstream. The vector construct was bombarded into tomato leaf calli and allowed to develop. We thus generated recombinant tomato plants preferentially expressing a Tat-GUS fusion protein over a Tat-only protein. In addition, plants bombarded with either *tat* or *mtat* genes showed no phenotypic difference and produced 2–4 μg Tat-GUS fusion protein per milligram soluble plant protein. Furthermore, tomato extracts intradermally inoculated into mice were found to induce a humoral and, most importantly, cellular immunity.

Keywords AIDS · Antibody response · Cellular immune response · HIV-1 · Tat · Transgenic tomato

M. E. Cueno · Y. Hibi · K. Imai · T. Okamoto (✉)
Department of Molecular and Cellular Biology, Molecular and Cellular Biology Laboratory, Graduate School of Medical Sciences, Nagoya City University, 1 Kawasumi, Misuho-cho, Mizuho-ku, Nagoya, Aichi 467-8601, Japan
e-mail: tokamoto@med.nagoya-cu.ac.jp

K. Karamatsu · Y. Yasutomi
Laboratory of Immunoregulation and Vaccine Research, Tsukuba Primate Research Center, National Institute of Biomedical Innovation, Tsukuba, Ibaraki 305-0843, Japan

A. C. Laurena
Biochemistry Laboratory, Institute of Plant Breeding, University of the Philippines Los Banos, Laguna 4031, Philippines

Introduction

HIV-1 has already claimed millions of victims worldwide and despite billions of dollars spent on HIV-1/AIDS research annually (Walker and Burton 2008; Watkins et al. 2008), no promising candidate HIV-1 vaccine has been made to date due to: (a) specific viral characteristics including extreme genetic variability among various isolates collected worldwide and even within the infected individuals; (b) a high mutation rate allowing rapid escape of variants from immune responses; and (c) biological properties of HIV-1 regulatory proteins, such as Nef and Tat, which avoid immune responses (Walker and Burton 2008; Watkins et al. 2008; WHO 2008; Potts et al. 2008). As widely believed, these characteristics pose a major obstacle towards controlling AIDS (Gaschen et al. 2002; Moore et al. 2008).

An ideal strategy against HIV-1 is one that stimulates passive protection or neutralizing immunity by producing both antibodies and cytotoxic T lymphocytes or CTLs (Walker and Burton 2008; Watkins et al. 2008; Addo et al. 2001). Earlier works have shown that CTLs can control HIV-1 replication in the absence of antibodies (Borrow et al. 1994) prompting several attempts to stimulate anti-viral CTL responses using a combination of varying HIV-1 proteins and their epitopes (Betts et al. 2005; Matano et al. 2004; Mwau et al. 2004). The Tat protein has been one of the well studied HIV-1 proteins (Barboric and Peterlin 2005; Emerman and Malim 1998; Goldstein et al. 2001; Okamoto and Wong-Staal 1986; Ramirez et al. 2007). It is a small regulatory protein composed of either 86 or 101 amino acid residues (14 or 18 kDa, respectively) encoded by two exons (Okamoto 1995). Among the HIV-1 proteins already studied, Tat shows great potential for CTL induction covering a wide variety of HIV-1 clones besides from little variability among distinct viral subtypes and is highly conserved in both inter- and intra-patient variants (Addo et al. 2001; Goldstein et al. 2001).

Over 4 million people become infected with HIV-1 each year (WHO 2008; Fox 2007) in third-world countries in particular (Flexner 2008). Cheap and affordable production of pharmaceutical products for third-world consumption has prompted the development of plant-made pharmaceuticals for often neglected diseases (Zahn et al. 2008), including HIV-1 (Ramirez et al. 2007; Flexner 2008; Shchelkunov et al. 2006; Webster et al. 2005). Previous attempts to utilize the tomato plant for HIV-1 Tat vaccine development in the form of an edible-vaccine was only successful in inducing antibodies or humoral immune response (Ramirez et al. 2007; Shchelkunov et al. 2006). At present, no report has been made with regards to induction of CTLs or cellular immune responses using Tat protein (Addo et al. 2001), more so, using a plant-expressed Tat protein.

In this study, we demonstrate the evidence of preferential expression of a Tat-GUS fusion protein over the Tat-only protein in tomato plant and is expressed much higher than previously reported (Ramirez et al. 2007). In addition, we were able to induce both humoral immune response and, surprisingly, cellular immune response using Balb/c mice when tomato extracts were intradermally introduced. To our knowledge, this is the first report of cellular immune induction using Tat expressed in a plant system.

Materials and methods

Vector construction and tomato transformation

The *tat* gene from the HXB2 strain of HIV-1 and *mtat* were synthesized following a specific codon-usage table based on tomato was used (www.kazusa.or.jp/codon/cgi-bin/showcodon.cgi?species=4081). The plant-optimized M2 epitope directly fused to either *tat* or inactive *mtat* (Imai et al. 2005) genes with a stop codon, were individually ligated into a pBI121 expression vector (Clontech) upstream of a *gusA* gene (Fig. 1). Transformation was performed using a particle gun

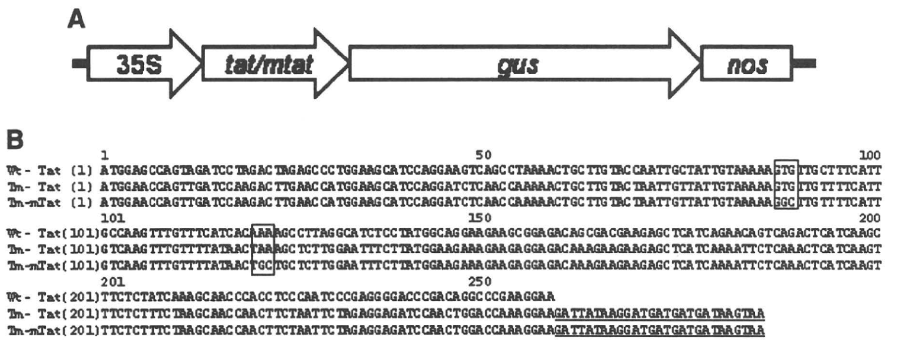

Fig. 1 Construction of the pBI121 plant expression vector containing either *tat* or *mtat* indirectly fused to *gusA* gene. **a** Expression was driven by 35S CaMV promoter and terminated with NOS termination signal located downstream of *gusA* gene. The inserted *tat*/*mtat* gene is located upstream of the *gusA* gene containing the termination codon (TAA) in between. **b** Codon-optimized *tat* and *mtat* were synthesized following the codon usage of tomato. The *boxed regions* represent point mutations at Cys30Ala and Lys41Ala found in *mtat* [23]. The *underlined segment* represents M2 epitope added to serve as an expression tag. Wt-Tat represents the Tat sequence from the HXB2 strain. Tm-Tat and Tm-mTat represents codon-optimized tomato Tat and mTat, respectively